catalysts

MDPI

Article

Radical C–H ^{18}F-Difluoromethylation of Heteroarenes with [^{18}F]Difluoromethyl Heteroaryl-Sulfones by Visible Light Photoredox Catalysis

Agostinho Luís Pereira Lemos [1,*,†], Laura Trump [1,2,†], Bénédicte Lallemand [2], Patrick Pasau [2], Joël Mercier [2], Christian Lemaire [1], Jean-Christophe Monbaliu [3], Christophe Genicot [2,*] and André Luxen [1,*]

1 GIGA-Cyclotron Research Centre In Vivo Imaging, University of Liège, 8 Allée du Six Août, Building B30, Sart Tilman, 4000 Liège, Belgium; laura.trump@ucb.com (L.T.); christian.lemaire@uliege.be (C.L.)
2 Global Chemistry, UCB NewMedicines, UCB Biopharma SPRL, 1420 Braine-l'Alleud, Belgium; benedicte.lallemand@ucb.com (B.L.); patrick.pasau@ucb.com (P.P.); joel.mercier@ucb.com (J.M.)
3 Center for Integrated Technology and Organic Synthesis, Research Unit MolSys, University of Liège, (Sart Tilman), B-4000 Liège, Belgium; jc.monbaliu@uliege.be
* Correspondence: agostinholemos43@gmail.com (A.L.P.L.); christophe.genicot@ucb.com (C.G.); aluxen@uliege.be (A.L.); Tel.: (+32)499509436 (A.L.P.L.)
† The authors contributed equally to this work.

Received: 5 February 2020; Accepted: 21 February 2020; Published: 1 March 2020

Abstract: The ^{18}F-labeling of CF_2H groups has been recently studied in radiopharmaceutical chemistry owing to the favorable nuclear and physical characteristics of the radioisotope ^{18}F for positron emission tomography (PET). Following up on the reported efficiency of the [^{18}F]difluoromethyl benzothiazolyl-sulfone (**[^{18}F]1**) as a ^{18}F-difluoromethylating reagent, we investigated the influence of structurally-related [^{18}F]difluoromethyl heteroaryl-sulfones in the reactivity toward the photoredox C–H ^{18}F-difluoromethylation of heteroarenes under continuous-flow conditions. In the present work, six new [^{18}F]difluoromethyl heteroaryl-sulfones **[^{18}F]5a**–**[^{18}F]5f** were prepared and, based on the overall radiochemical yields (RCYs), three of these reagents (**[^{18}F]5a**, **[^{18}F]5c**, and **[^{18}F]5f**) were selected for the fully automated radiosynthesis on a FASTlab^{TM} synthesizer (GE Healthcare) at high level of starting radioactivity. Subsequently, their efficiency as ^{18}F-difluoromethylating reagents was evaluated using the antiherpetic drug acyclovir as a model substrate. Our results showed that the introduction of molecular modifications in the structure of **[^{18}F]1** influenced the amount of *fac*-$Ir^{III}(ppy)_3$ and the residence time needed to ensure a complete C–H ^{18}F-difluoromethylation process. The photocatalytic C–H ^{18}F-difluoromethylation reaction with the reagents **[^{18}F]5a**, **[^{18}F]5c**, and **[^{18}F]5f** was extended to other heteroarenes. Radical-trapping experiments demonstrated the likely involvement of radical species in the C–H ^{18}F-difluoromethylation process.

Keywords: fluorine-18; difluoromethylation; heteroarenes; visible light; photocatalysis

1. Introduction

The fluorine-18 (^{18}F) isotope has been regarded the "radionuclide of choice" due to its suitable physical and nuclear features for in vivo positron emission tomography (PET) imaging in living subjects [1–4]. The unique sensitivity of PET makes this technique appropriate for the study of absorption, distribution, metabolism, and excretion (ADME) properties of radiopharmaceuticals and the evaluation of their pharmacodynamic profile. In addition, PET technology has proven highly valuable in the observation of biochemical and physiological changes that may take place before the anatomical alterations of a certain disease are detected [5–8]. The suitability of the ^{18}F radioisotope in

PET has encouraged radiochemists to invest much effort in the development of efficient ^{18}F-fluorination and ^{18}F-fluoroalkylation strategies [9–19].

Among the existent fluorinated motifs, the difluoromethyl (CF_2H) group has recently attracted considerable attention in medicinal chemistry due to its lipophilic hydrogen-bond donor properties [20–24]. The CF_2H substitution may offer a viable alternative to conventional hydrogen-bond donors (e.g., hydroxy (OH) and thiol (SH) groups) in terms of lipophilicity, cell membrane permeability, and metabolic stability, thus modulating the pharmacological activity of pharmaceuticals and agrochemicals [25–31]. Despite the recent progresses in the preparation of CF_2H-containing derivatives in organofluorine chemistry, methodologies for the ^{18}F-labeling of CF_2H groups are still relatively scarce. Most labeling strategies relied on the radiosynthesis of [^{18}F]aryl–CF_2H derivatives *via* ^{18}F-fluorination of suitable precursors with the electrophilic reagent [^{18}F]Selectfluor *bis*(triflate) [32] or with the cyclotron-produced [^{18}F]fluoride by aliphatic nucleophilic substitution [33–36]. Furthermore, the resulting [^{18}F]aryl–CF_2H derivatives are afforded in low-to-moderate molar activities (up to 22 GBq·μmol^{-1}). The production of radiotracers with high molar activity is mandatory for PET imaging studies, especially for targeting low-density biomacromolecules. Recently, we disclosed an innovative method reporting the photoredox late-stage C–H ^{18}F-difluoromethylation of *N*-containing heteroarenes with the [^{18}F]difluoromethyl benzothiazolyl-sulfone (**[^{18}F]1**) with improved molar activity [A_m (**[^{18}F]1**) = 54 ± 7 GBq·μmol^{-1}] [37,38] (Figure 1A). In non-radioactive chemistry, difluoromethyl heteroaryl-sulfones have been widely implemented in photoredox catalyzed C–H difluoromethylation processes because of the ability of these compounds to be reduced to CF_2H radicals in the presence of appropriate photocatalysts in their photoexcited state. In 2016, Hu and Fu reported the use of difluoromethyl benzothiazolyl-sulfone (**1**) in the radical C–H difluoromethylation of biphenyl isocyanides [39] and olefinic amides [40], respectively. The reagent **1** was also employed in the preparation of CF_2H–substituted heterocycles of biological relevance, including isoquinolinediones [41], coumarins [42], isoxazolines [43], and oxindoles [44]. In 2019, Liu and co-workers developed a procedure for C–H difluoromethylation of *N*-arylacrylamides with the reagent difluoromethyl pyridyl-sulfone (**2**), under visible light photoredox conditions [45] (Figure 1B).

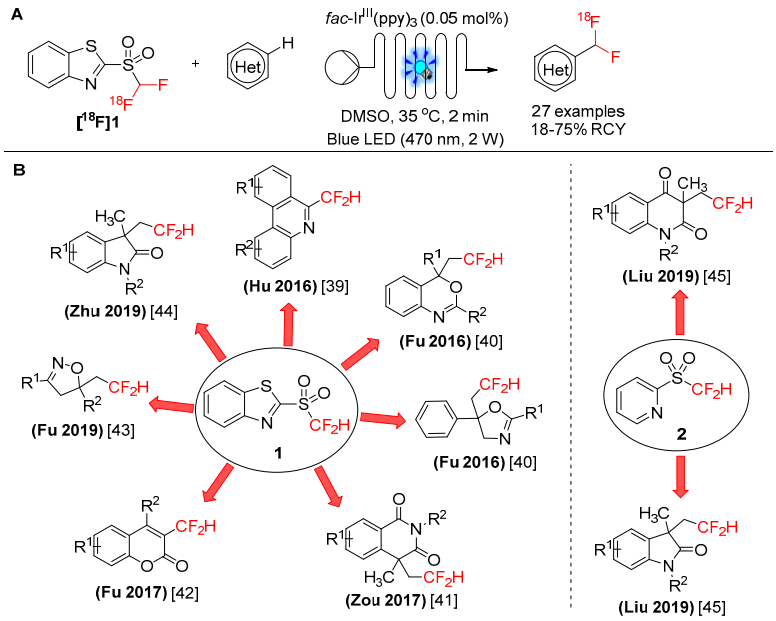

Figure 1. (**A**) Photoredox C–H ^{18}F-difluoromethylation of *N*-containing heteroarenes with [^{18}F]difluoromethyl benzothiazolyl-sulfone (**[^{18}F]1**), under continuous-flow conditions [37,38]. (**B**) Application of the difluoromethyl sulfones **1** and **2** in the preparation of heterocycles of biological relevance, under visible light photoredox catalysis [39–45].

Based on the effectiveness of the sulfone **[^{18}F]1** as ^{18}F-difluoromethylating reagent [37,38], we intended to study the influence of certain molecular modifications in the structure of **[^{18}F]1** on the reactivity towards the C–H ^{18}F-difluoromethylation of *N*-heteroaromatics. The molecular modifications consisted in the introduction of a single electron-donating (OCH_3) (Figure 2A) or electron-withdrawing (NO_2) substituent (Figure 2B) either at position 5 or 6 of the benzothiazolyl ring and in the alteration of the original benzothiazolyl moiety to other heteroaryl rings (*N*-methyl-benzimidazolyl and *N*-phenyl-tetrazolyl rings) (Figure 2C). In this work, we opted to perform the radiosyntheses of structurally-related [^{18}F]difluoromethyl heteroaryl-sulfones and subsequently evaluate their efficiency in the photoredox C–H ^{18}F-difluoromethylation of heteroarenes, under continuous-flow conditions as reported previously [37]. To the best of our knowledge, the effectiveness of the non-radioactive references of these novel [^{18}F]difluoromethyl heteroaryl-sulfones in photoredox C–H difluoromethylation has never been described in the literature.

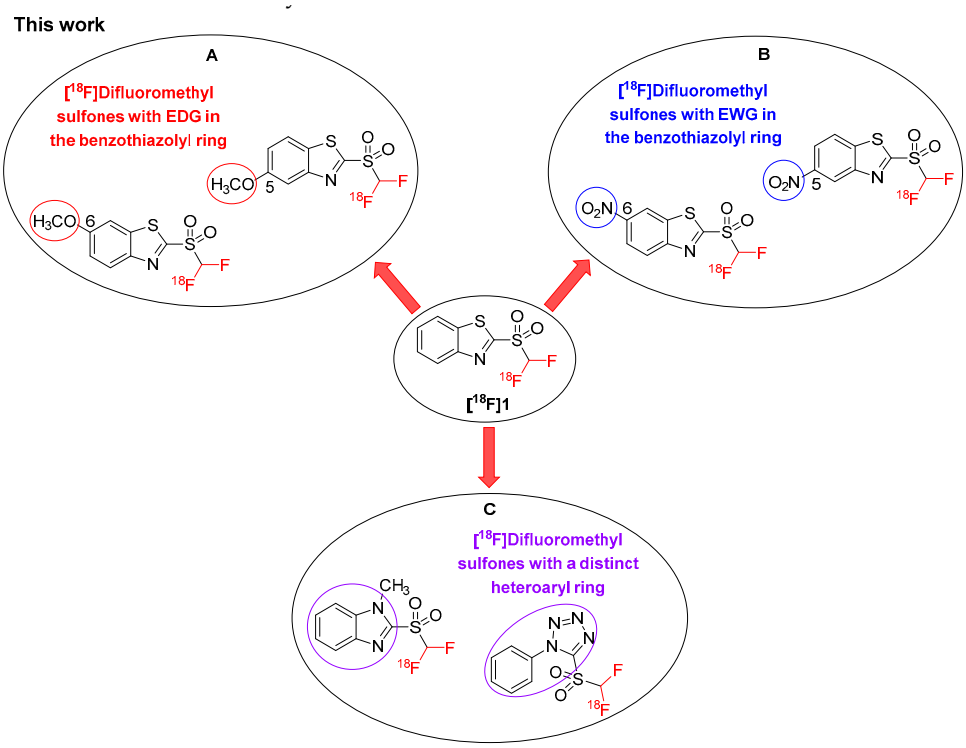

Figure 2. Molecular modifications performed on **[^{18}F]1**: introduction of a single electron-donating (OCH_3) (**A**) or electron-withdrawing (NO_2) (**B**) substituent either at position 5 or 6 of the benzothiazolyl ring, and modification of the original benzothiazolyl moiety to other heteroaryl rings (**C**).

2. Results and Discussion

2.1. Chemistry

Synthesis of the Difluoromethyl Heteroaryl-Sulfones **5a**–**5f**

We initially performed the organic synthesis of the difluoromethyl heteroaryl-sulfones **5a**–**5f** as non-radioactive standards for confirmation of the identity of the ^{18}F-labeled compounds. In order to prepare the difluoromethyl heteroaryl-sulfones **5a**–**5f**, we considered a two-step procedure involving the difluoromethylation of the heteroaryl-thiols **3a**–**3f** to afford the difluoromethyl heteroaryl-sulfides **4a**–**4f**. Oxidation of the sulfides **4a**–**4f** would lead to the sulfones **5a**–**5f** (Scheme 1).

Inspired by the methodologies formerly described by Akita [46] and Jubault [47], the difluoromethylation of the heteroaryl-thiols **3a**–**3f** using sodium chlorodifluoroacetate ($ClCF_2CO_2Na$) and potassium carbonate (K_2CO_3) provided the corresponding sulfides **4a**–**4f** in moderate yields

(Scheme 1, 18–58% yields). The difluoromethyl heteroaryl-sulfones **5a**–**5f** were successfully achieved by oxidation of the sulfides **4a**–**4f** using the oxidizing agent sodium (meta)perioiodate ($NaIO_4$) and ruthenium (III) chloride hydrate ($RuCl_3{\cdot}xH_2O$) (Scheme 1, 64–87% yields).

The structure elucidation of the compounds **4a**–**4f** and **5a**–**5f** was established on the basis of high-resolution mass spectrometry (HRMS) and nuclear magnetic resonance (NMR) techniques (Figures S1–S36).

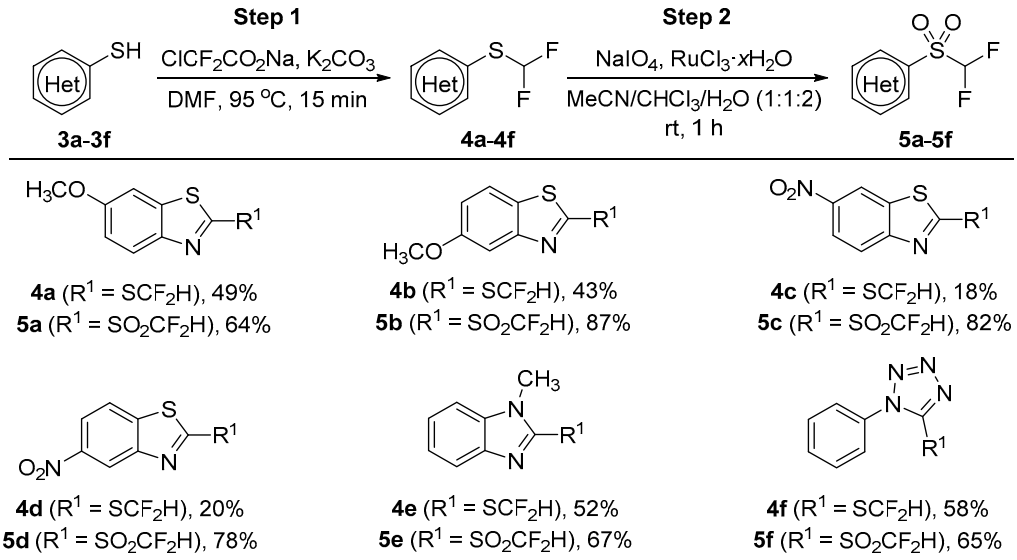

Scheme 1. Synthesis of the difluoromethyl heteroaryl-sulfides **4a**–**4f** and the heteroaryl-sulfones **5a**–**5f**. **Step 1**: **3a**–**3f** (3.0 mmol), sodium chlorodifluoroacetate (6.0 mmol), K_2CO_3 (4.5 mmol), DMF (10 mL), 95 °C, 15 min. **Step 2**: **4a**–**4f** (1.0 mmol), sodium (meta)periodate (5.0 mmol), ruthenium (III) chloride hydrate (0.05 mmol), MeCN (2 mL), $CHCl_3$ (2 mL), H_2O (4 mL), rt, 1 h. All reaction yields are of isolated products.

2.2. Radiochemistry

2.2.1. Radiosyntheses of the [^{18}F]Difluoromethyl Heteroaryl-Sulfones **[^{18}F]5a**–**[^{18}F]5f**

We planned the radiosyntheses of the sulfones **[^{18}F]5a**–**[^{18}F]5f** following a two-step methodology previously described in the literature [37]. This multi-step strategy involved the initial nucleophilic ^{18}F-fluorination of the bromofluoromethyl heteroaryl-sulfides **6a**–**6f** and subsequent oxidation of the [^{18}F]difluoromethyl heteroaryl-sulfides **[^{18}F]4a**–**[^{18}F]4f**. The precursors **6a**–**6f** were prepared by a one-step bromofluoromethylation of the heteroaryl-thiols **3a**–**3f** with dibromofluoromethane (Br_2CFH), under basic conditions (see *Materials and Methods* section for more details). The structure elucidation of the compounds **6a**–**6f** was established on the basis of HRMS and NMR techniques (Figures S37–S54). Low starting radioactivity experiments were performed in order to investigate the propensity of the newly synthesized precursors to undergo the expected nucleophilic ^{18}F-fluorination, under the same ^{18}F-labeling conditions used to prepare the [^{18}F]difluoromethyl benzothiazolyl-sulfide (**[^{18}F]1′**) [37]. To minimize the radiation exposure, the ^{18}F-labeling reactions were conducted in a commercially available FASTlab^{TM} module (GE Healthcare) placed in a shielded hotcell. An aliquot of a solution of [^{18}F]fluoride in [^{18}O]water ([^{18}O]H_2O) (150–200 MBq) was passed through a quaternary methyl ammonium (QMA) carbonate cartridge for [^{18}F]fluoride trapping. Subsequent elution of the [^{18}F]fluoride using $K_{2.2.2}/K_2CO_3$-based eluent and azeotropic drying in a cyclic olefin copolymer (COC) reactor furnished the "naked" [^{18}F]fluoride readily available for the nucleophilic ^{18}F-fluorination. Precursors **6c** (0.02 mmol) and **6a, 6b, 6d**–**6f** (0.04 mmol) in acetonitrile (MeCN, 1 mL) were added to the dry [^{18}F]fluoride and the ^{18}F-labeling reaction was conducted at 120 °C for 5 min. The crude reaction mixture was pre-purified using a Sep-Pak® C18 Plus Short cartridge to eliminate the unreacted

[^{18}F]fluoride and other polar impurities. Only for radiochemical yield (RCY) determination, the cartridge-purified **[^{18}F]4a**–**[^{18}F]4f** were then eluted with MeCN (Scheme 2: 6 examples, 8.3–14.8% RCY (decay-corrected at the start-of-synthesis (SOS)). No significant differences in RCYs of the radiosyntheses of the cartridge-purified **[^{18}F]1′** and **[^{18}F]4a**–**[^{18}F]4f** were remarked. These results suggest that the introduction of either electron-donating or electron-withdrawing groups on the benzothiazolyl ring, or the alteration of the original benzothiazolyl moiety to other heteroaryl rings did not have a meaningful impact in the reactivity of the precursors toward the ^{18}F-labeling reaction.

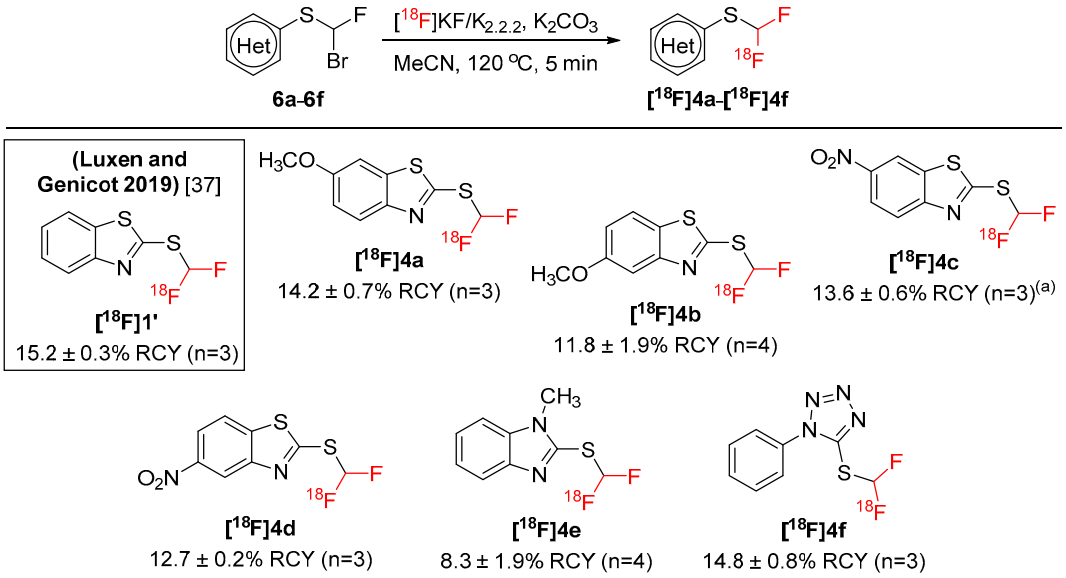

Scheme 2. Radiosyntheses of [^{18}F]difluoromethyl heteroaryl-sulfides (**[^{18}F]4a**–**[^{18}F]4f**). Standard conditions: **6a**, **6b**, **6d**–**6f** (0.04 mmol), [^{18}F]KF (150–200 MBq), K_2CO_3 (0.01 mmol), $K_{2.2.2}$ (0.02 mmol), MeCN (1 mL), 120 °C, 5 min. [(a)] ^{18}F-Labeling reaction of **6c** was performed on a 0.02 mmol scale. All radiochemical yields (RCYs) were determined based on the activity of cartridge-purified **[^{18}F]4a**–**[^{18}F]4f**, their radio-thin layer chromatography (radio-TLC) and their radio-ultra performance liquid chromatography (radio-UPLC) purities, and the starting radioactivity. All RCYs were decay-corrected at the start-of-synthesis (SOS).

Afterward, the oxidation of the cartridge-purified **[^{18}F]4a**–**[^{18}F]4f** was undergone in the Sep-Pak® C18 Plus Short cartridge, upon the addition of an aqueous solution of the $NaIO_4$ and $RuCl_3{\cdot}xH_2O$, at room temperature for 5 min. Based on the previously reported oxidation conditions for the radiosynthesis of **[^{18}F]1** (Table 1, Entry 1) [37], the labeled compound **[^{18}F]5a** was synthesized from the cartridge-purified **[^{18}F]4a** in 32.1% RCY (Table 1, Entry 2). However, no complete conversion of **[^{18}F]4a** was observed. Optimization studies were then conducted to uncover the most suitable reaction conditions to achieve the complete oxidation of **[^{18}F]4a**. A two-fold increase in the amount of $RuCl_3{\cdot}xH_2O$ resulted in a significant improvement of the oxidation efficiency (Table 1, Entry 3). By raising the amount of $NaIO_4$ from 0.24 mmol to 0.72 mmol, the **[^{18}F]4a** was fully consumed and the labeled compound **[^{18}F]5a** was isolated in 70.9 ± 6.1% RCY, after cartridge purification (Table 1, Entry 4).

Table 1. Optimization of the oxidation conditions of the **[^{18}F]4a**[(a)].

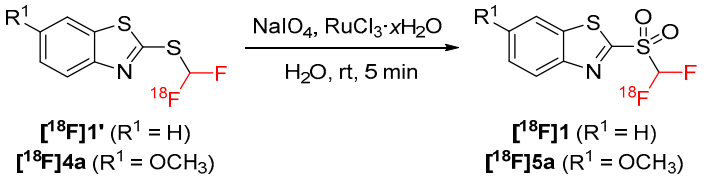

Entry	Substrate	$NaIO_4$ (mmol)	$RuCl_3{\cdot}xH_2O$ (mmol)	Conversion (%)[(b)]	RCY (%)[(c)]
1	**[^{18}F]1′**	0.24	0.008	100	82.9 ± 7.9 (n = 3)
2	**[^{18}F]4a**	0.24	0.008	35	32.1
3	**[^{18}F]4a**	0.24	0.016	64	59.6
4	**[^{18}F]4a**	0.72	0.016	100	70.9 ± 6.1 (n = 3)

[(a)] Standard conditions: $NaIO_4$, $RuCl_3{\cdot}xH_2O$, H_2O (1 mL), rt, 5 min. [(b)] UPLC conversion of the substrate **[^{18}F]4a**. [(c)] All RCYs were determined based on the activity of cartridge-purified **[^{18}F]4a** and **[^{18}F]5a**, their radio-TLC and their radio-UPLC purities. All RCYs were decay-corrected at the SOS.

With the optimized conditions in hand, the oxidation protocol was extended to the other [^{18}F]difluoromethyl heteroaryl-sulfides (**[^{18}F]4b**–**[^{18}F]4f**), furnishing the labeled compounds **[^{18}F]5b**–**[^{18}F]5f** in good-to-excellent RCY (70.6–91.9% RCY, Scheme 3). The ultra performance liquid chromatography (UPLC) retention times of the labeled compounds **[^{18}F]4a**–**[^{18}F]4f** (Figures S56–S67) and **[^{18}F]5a**–**[^{18}F]5f** (Figures S69–S80) were compliant with those of the respective non-radioactive authentic references.

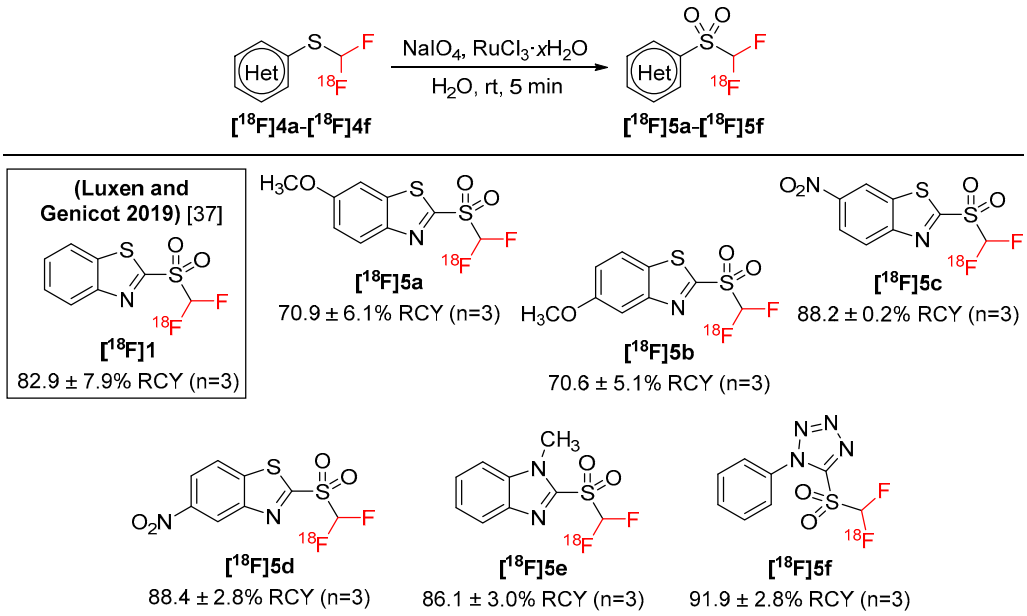

Scheme 3. Radiosyntheses of [^{18}F]difluoromethyl heteroaryl-sulfones (**[^{18}F]5a**–**[^{18}F]5f**). Standard conditions: **[^{18}F]4a**–**[^{18}F]4f** (10–20 MBq), sodium (meta)periodate (0.72 mmol), ruthenium (III) chloride hydrate (0.016 mmol), H_2O (1 mL), rt, 5 min. All RCYs were determined based on the activity of cartridge-purified **[^{18}F]4a**–**[^{18}F]4f** and **[^{18}F]5a**–**[^{18}F]5f**, their radio-TLC and their radio-UPLC purities. All RCYs were decay-corrected at the SOS.

According to the results presented in Table 2, the best RCYs for the two-step radiosyntheses of the cartridge-purified **[^{18}F]5a**–**[^{18}F]5f** at low level of starting radioactivity (90–150 MBq) were attained with the electron-rich benzothiazolyl derivative **[^{18}F]5a** [RCY (**[^{18}F]5a**) > RCY (**[^{18}F]5b**), Table 2], the electron-poor derivative **[^{18}F]5c** [RCY (**[^{18}F]5c**) > RCY (**[^{18}F]5d**), Table 2], and the *N*-phenyl-tetrazolyl derivative **[^{18}F]5f** [RCY (**[^{18}F]5f**) > RCY (**[^{18}F]5e**), Table 2]. These compounds were then selected for the investigation of their reactivity towards the photocatalytic ^{18}F-difluoromethylation of *N*-containing

heteroarenes. In order to circumvent any potential radioprotection issues, a fully automated process involving the two-step radiosyntheses of **[^{18}F]5a**, **[^{18}F]5c**, or **[^{18}F]5f** and a high performance liquid chromatography (HPLC) purification was implemented on a FASTlab^{TM} synthesizer (GE Healthcare) for the preparation of the purified ^{18}F-labeled compounds.

Table 2. Two-step radiosyntheses of the **[^{18}F]5a**–**[^{18}F]5f** from the precursors **6a**–**6f**.

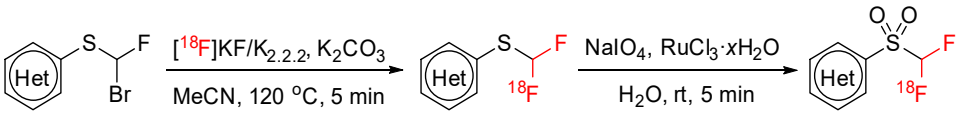

Entry	[^{18}F]Difluoromethyl Heteroaryl-Sulfones	RCY (%)[(a)]
1	**[^{18}F]5a**	10.1 ± 0.8 (n = 3)
2	**[^{18}F]5b**	8.3 ± 0.6 (n = 3)
3	**[^{18}F]5c**	12 ± 0.5 (n = 3)
4	**[^{18}F]5d**	11.2 ± 0.3 (n = 3)
5	**[^{18}F]5e**	7.2 ± 0.2 (n = 3)
6	**[^{18}F]5f**	13.6 ± 0.4 (n = 3)

[(a)] All RCYs were determined based on the activity of cartridge-purified **[^{18}F]5a**–**[^{18}F]5f**, their radio-TLC, their radio-UPLC purities, and the starting radioactivity. All RCYs were decay-corrected at the SOS.

2.2.2. Automated Radiosyntheses of the [^{18}F]Difluoromethyl Heteroaryl-Sulfones **[^{18}F]5a**, **[^{18}F]5c**, and **[^{18}F]5f**

The automated sequence for the radiosyntheses of **[^{18}F]5a**, **[^{18}F]5c**, and **[^{18}F]5f** involved the following steps: (1) machine and cassette tests (presynthesis, 7 min); (2) [^{18}F]fluoride recovery, trapping, elution, and azeotropic drying (12 min); (3) transfer of the precursors **6a**, **6c**, and **6f** to the reactor and ^{18}F-labeling (9 min); (4) dilution of the crude product **[^{18}F]4a**, **[^{18}F]4c**, and **[^{18}F]4f** with water, and trapping on a ^{t}C18 Plus Short cartridge (2 min); (5) transfer of the $NaIO_4$ and $RuCl_3{\cdot}xH_2O$ and oxidation on a ^{t}C18 cartridge (6 min); (6) elution of the crude **[^{18}F]5a**, **[^{18}F]5c**, and **[^{18}F]5f** with MeCN to the reactor, dilution with water, and injection on the semi-preparative HPLC loop (4 min); (7) HPLC purification and collection of the purified **[^{18}F]5a** (26 min), **[^{18}F]5c** (23 min), and **[^{18}F]5f** (18 min); (8) dilution of the trapping on a ^{t}C18 Plus Short cartridge followed by elution with anhydrous dimethyl sulfoxide (DMSO) (14 min). A more detailed description of the sequence of events comprising the multi-step radiosyntheses of the **[^{18}F]5a**, **[^{18}F]5c**, and **[^{18}F]5f** is provided in the *Materials and Methods* section. The reagents and materials used throughout the radiochemical process were prepared and positioned in the FASTlab^{TM} manifold as depicted in Table S23 and illustrated in Figure 3.

A HPLC purification of the crude **[^{18}F]5a**, **[^{18}F]5c**, and **[^{18}F]5f** was implemented on a reverse-phase HPLC column. The purity of these newly synthesized compounds revealed to be critical for the examination of their efficiency towards the following photocatalytic ^{18}F-difluoromethylation reaction. In fact, during the radiosyntheses of the sulfones **[^{18}F]5a**, **[^{18}F]5c**, and **[^{18}F]5f**, the oxidation of the precursors **6a**, **6c**, and **6f** represented an important side reaction, leading to the formation of the corresponding bromofluoromethyl heteroaryl-sulfones (**6a′**, **6c′**, and **6f′**, Scheme 4). The use of a mobile phase of MeCN/H_2O (40/60, *v*/*v*) in isocratic mode enabled an effective separation between the radiotracers **[^{18}F]5a**, **[^{18}F]5c**, and **[^{18}F]5f** and the respective UV by-products, particularly the bromofluoromethyl heteroaryl-sulfones **6a′**, **6c′**, and **6f′**. The radioactive peaks corresponding to the radiotracers **[^{18}F]5a**, **[^{18}F]5c**, and **[^{18}F]5f** were collected after 22 min (Figure 4), 19 min (Figure 5), and 15 min (Figure 6), respectively, and formulated on the same FASTlab^{TM} cassette by using a preconditioned Sep-Pak® C18 Plus Short cartridge. The trapped **[^{18}F]5a**, **[^{18}F]5c**, and **[^{18}F]5f** were then eluted with anhydrous DMSO using reverse flow and recovered in a 4 mL-sealed vial.

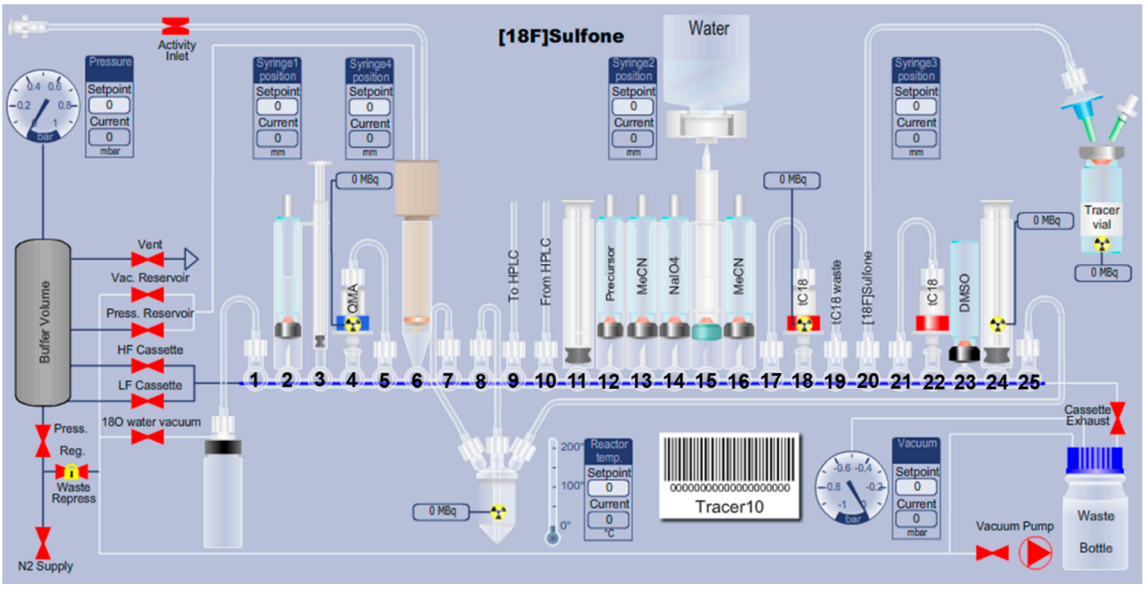

Figure 3. Layout of the FASTlab™ cassette for the radiosyntheses of the labeled compounds **[^{18}F]5a**, **[^{18}F]5c**, and **[^{18}F]5f**.

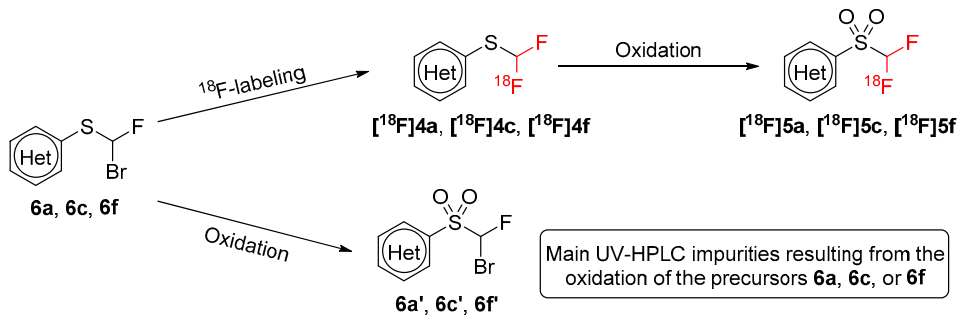

Scheme 4. Formation of the by-products **6a′**, **6c′**, and **6f′** by oxidation of the precursors **6a**, **6c**, and **6f**, respectively.

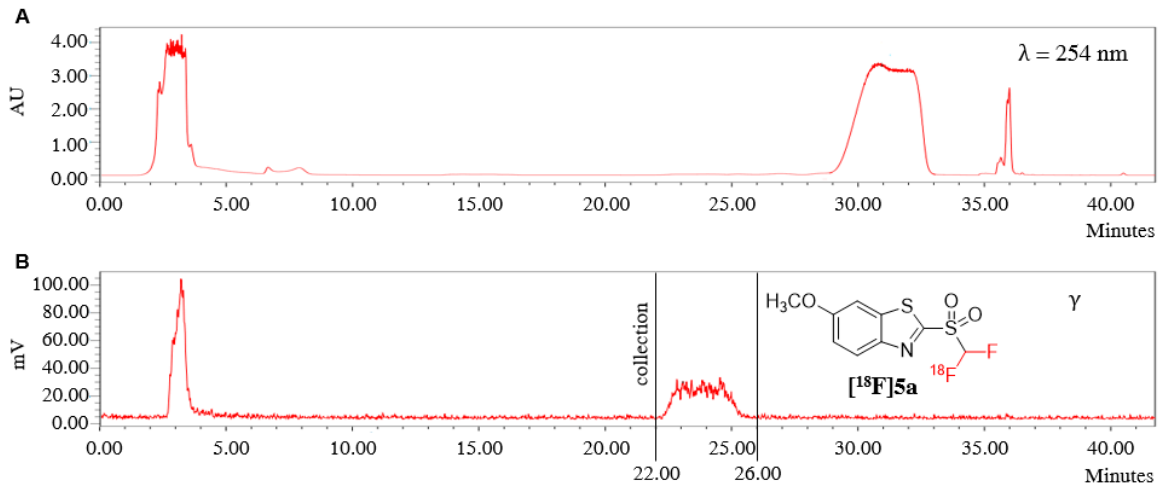

Figure 4. (**A**) Ultraviolet-high performance liquid chromatography (UV-HPLC) purification profile of the crude **[^{18}F]5a**. (**B**) Radio-HPLC purification profile of the crude **[^{18}F]5a**. Note: the appearance of broad flat-topped peaks in UV-HPLC chromatogram is derived from a saturation of the UV detector by the injecting crude product **[^{18}F]5a**.

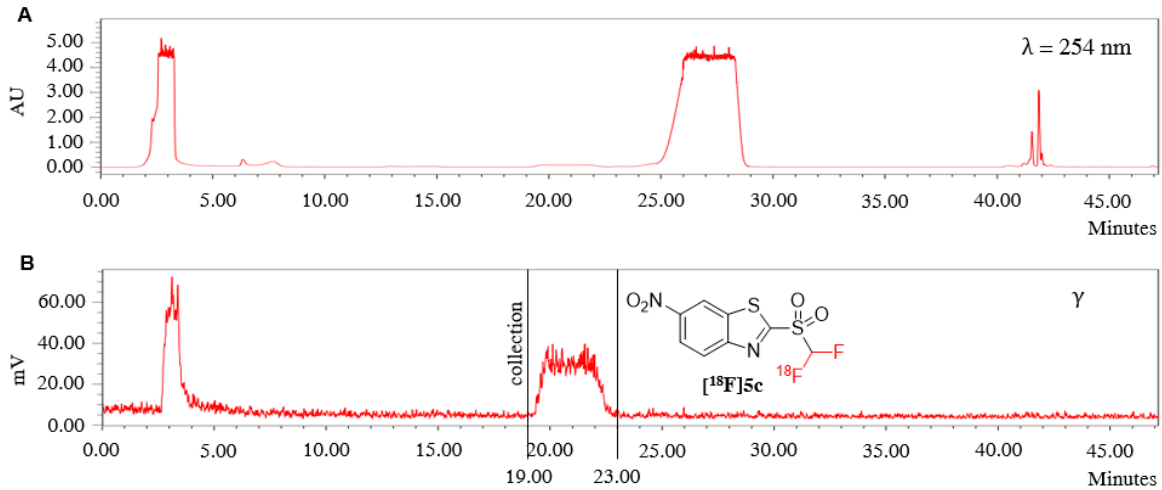

Figure 5. (**A**) UV-HPLC purification profile of the crude **[^{18}F]5c**. (**B**) Radio-HPLC purification profile of the crude **[^{18}F]5c**. Note: the appearance of broad flat-topped peaks in UV-HPLC chromatogram is derived from a saturation of the UV detector by the injecting crude product **[^{18}F]5c**.

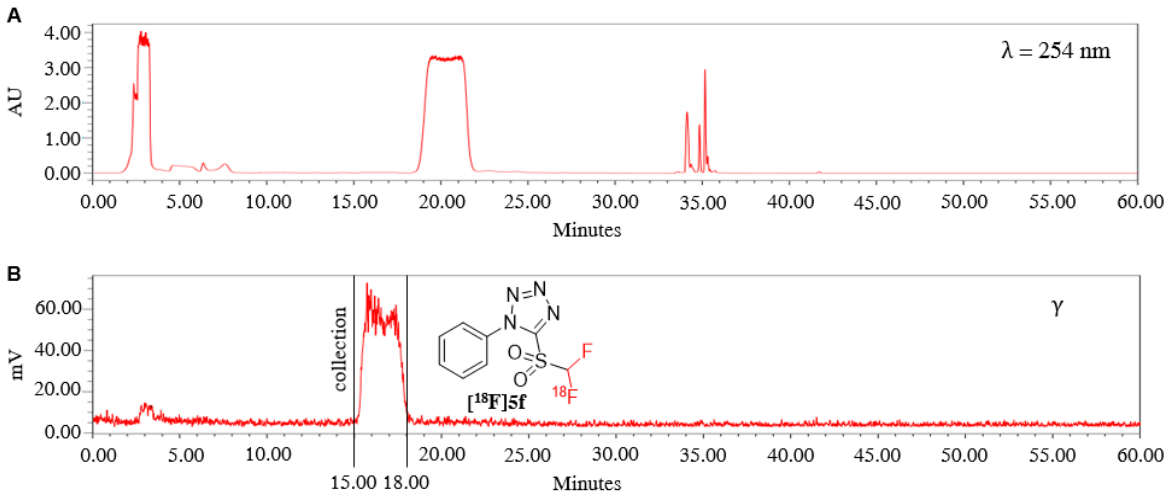

Figure 6. (**A**) UV-HPLC purification profile of the crude **[^{18}F]5f**. (**B**) Radio-HPLC purification profile of the crude **[^{18}F]5f**. Note: the appearance of broad flat-topped peaks in UV-HPLC chromatogram is derived from a saturation of the UV detector by the injecting crude product **[^{18}F]5f**.

The fully automated radiosyntheses of **[^{18}F]5a**, **[^{18}F]5c**, and **[^{18}F]5f** (^{18}F-labeling, oxidation, HPLC purification, and formulation) were performed in 73 min, 70 min, and 65 min, respectively. Starting from 125–150 GBq of [^{18}F]fluoride, the labeled compounds **[^{18}F]5a**, **[^{18}F]5c**, and **[^{18}F]5f** were isolated in 2.9 ± 0.1%, 5.7 ± 0.5%, and 8.0 ± 0.9% RCYs (decay-corrected at the SOS), respectively (Table 3). The RCY of each automated radiosynthesis was determined based on the ratio between the radioactivity of the **[^{18}F]5a**, **[^{18}F]5c**, or **[^{18}F]5f** present in the DMSO solution (decay-corrected at the SOS) and the radioactivity trapped on the QMA carbonate cartridge at the SOS.

Obtaining a high molar activity still constitutes a major challenge for the radiosyntheses of [^{18}F]CF_2H–bearing compounds, due to the unwanted ^{18}F–^{19}F isotopic exchange reactions. This fully automated methodology allowed the preparation of the **[^{18}F]5a**, **[^{18}F]5c**, and **[^{18}F]5f** with improved molar activities in comparison with the sulfone **[^{18}F]1** [A_m (**[^{18}F]5a**) = 139 ± 17 GBq·μmol^{-1} > A_m (**[^{18}F]5f**) = 113 ± 17 GBq·μmol^{-1} > A_m (**[^{18}F]5c**) = 62 ± 12 GBq·μmol^{-1} > A_m (**[^{18}F]1**) = 54 ± 7 GBq·μmol^{-1}, all A_m values in Table 3 were determined at the end of the synthesis (EOS)].

Table 3. Radiochemical yields and molar activities of the reagents **[^{18}F]5a**, **[^{18}F]5c**, and **[^{18}F]5f**.

Reagents	[^{18}F]5a	[^{18}F]5c	[^{18}F]5f
Duration of the radiosynthesis (min)	73	70	65
RCY (%)[(a)]	2.9 ± 0.1	5.7 ± 0.5	8.0 ± 0.9
Molar activity (GBq·μmol^{-1})[(b)]	139 ± 17	62 ± 12	113 ± 17

[(a)] All RCYs were determined based on the radioactivity of the **[^{18}F]5a**, **[^{18}F]5c**, or **[^{18}F]5f** present in the dimethyl sulfoxide (DMSO) solution (decay-corrected at the SOS) and the radioactivity trapped on the QMA carbonate cartridge at the SOS. [(b)] Molar activities were determined at the end of the synthesis (EOS).

2.2.3. ^{18}F-Difluoromethylation of Heteroarenes with Sulfones **[^{18}F]5a**, **[^{18}F]5c**, and **[^{18}F]5f**

Next, we evaluated the tendency of the newly synthesized [^{18}F]difluoromethyl heteroaryl-sulfones **[^{18}F]5a**, **[^{18}F]5c**, and **[^{18}F]5f** towards the C–H ^{18}F-difluoromethylation of *N*-containing heteroarenes, under irradiation with blue light-emitting diode (LED) (470 nm, 2 W). The C–H ^{18}F-difluoromethylation reactions were performed in continuous-flow using an easy-to-use platform equipped with a 100 μL microreactor made from glass and a syringe that continuously pumps the reaction mixture into the microreactor at a given flow rate (FlowStart Evo, FutureChemistry, Nijmegen, The Netherlands) (Figure S85). The use of a continuous-flow system assures an efficient irradiation of the reaction mixture during the photocatalytic processes and can potentially lead to an enhanced productivity in significantly reduced reaction times [37]. The reaction time is a relevant parameter in ^{18}F-radiochemistry. We initially explored the reactivity of the sulfones **[^{18}F]5a**, **[^{18}F]5c**, and **[^{18}F]5f** for the C–H ^{18}F-difluoromethylation of the antiherpetic drug acyclovir (**7e**) [48] under the reaction conditions recently reported in our laboratories (Table 4, Entry 1) [37]. The visible light-mediated C–H ^{18}F-difluoromethylation of **7e** with the sulfones **[^{18}F]5a**, **[^{18}F]5c**, and **[^{18}F]5f** was conducted at 35 °C in DMSO, in the presence of the photocatalyst *fac*-Ir^{III}(ppy)$_3$ (0.05 mol %), and with a residence time of 2 min (flow rate = 50 μL·min^{-1}). Under these conditions, the reagents **[^{18}F]5a**, **[^{18}F]5c**, and **[^{18}F]5f** revealed to be competent substrates for the C–H ^{18}F-difluoromethylation of **7e**, affording the [^{18}F]acyclovir–CF$_2$H (**[^{18}F]8e**) in 57 ± 7% (Table 4, Entry 2), 14 ± 1% (Table 4, Entry 3), and 48 ± 8% RCYs (Table 4, Entry 6), respectively. Regardless of the employed ^{18}F-difluoromethylating reagent, the labeled compound **[^{18}F]8e** was furnished in lower RCYs, in comparison with the sulfone **[^{18}F]1** (Table 4, Entry 1). Among the tested reagents, only **[^{18}F]5a** was fully consumed after the present photocatalytic reaction. Raising the amount of *fac*-Ir^{III}(ppy)$_3$ and the residence time demonstrated to be beneficial for the efficiency of the sulfones **[^{18}F]5c** and **[^{18}F]5f** toward the C–H ^{18}F-difluoromethylation of **7e**. Regarding the sulfone **[^{18}F]5c**, a ten-fold increase of the amount of photocatalyst (0.5 mol%) led to the formation of the product **[^{18}F]8e** in 26 ± 3% RCY (Table 4, Entry 4). The duplication of the residence time (flow rate = 25 μL·min^{-1}) allowed a full consumption of **[^{18}F]5c** in the photochemical process and the obtention of **[^{18}F]8e** in 51 ± 7% RCY (Table 4, Entry 5). Changing the amount of photocatalyst from 0.05 mol% to 0.1 mol % and the residence time from 2 min (flow rate = 50 μL·min^{-1}) to 2.5 min (flow rate = 40 μL·min^{-1}) enabled the complete consumption of the reagent **[^{18}F]5f** and resulted in the production of **[^{18}F]8e** in 56 ± 1% RCY (Table 4, Entry 8). These results demonstrated that a single introduction of the –NO$_2$ group (an electron-withdrawing substituent) at position 6 and the alteration of the benzothiazolyl ring of **[^{18}F]1** to the *N*-phenyl-tetrazolyl moiety yielded ^{18}F-difluoromethylating reagents with lower reactivity for the C–H ^{18}F-difluoromethylation of **7e** in comparison with the sulfone **[^{18}F]1**. Overall, the introduction of molecular modifications in the structure of **[^{18}F]1** can modulate the reactivity of the resulting ^{18}F-difluoromethylating reagents, influencing the amount of the photocatalyst *fac*-Ir^{III}(ppy)$_3$ and the residence time necessary to assure a complete C–H ^{18}F-difluoromethylation reaction.

Table 4. Optimization of the conditions for the C–H ^{18}F-difluoromethylation of acyclovir (**7e**) with the reagents **[^{18}F]5a**, **[^{18}F]5c**, and **[^{18}F]5f**[(a)].

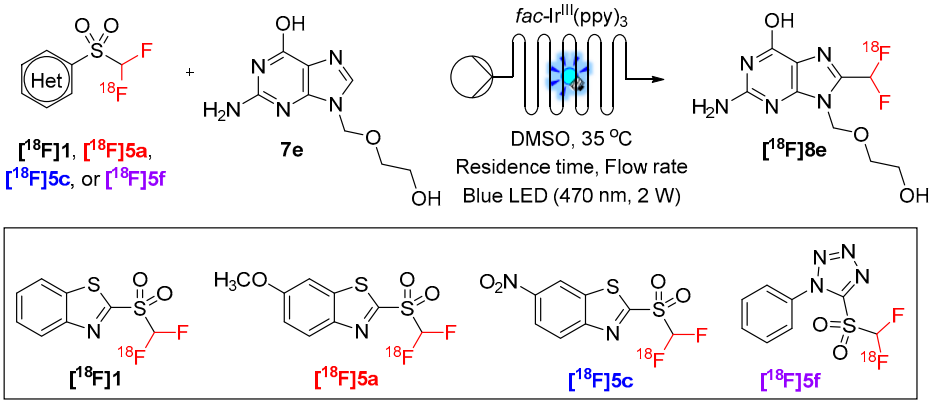

Entry	Reagents	*fac*-Ir^{III}(ppy)$_3$ (mol%)	Residence Time (min)	Flow Rate (μL·min^{-1})	Conversion (%)[(b)]	RCY (%)[(c)]
1	**[^{18}F]1**	0.05	2	50	100	70 ± 7 (n = 4)
2	**[^{18}F]5a**	0.05	2	50	100	57 ± 7 (n = 3)
3	**[^{18}F]5c**	0.05	2	50	17	14 ± 1 (n = 3)
4	**[^{18}F]5c**	0.5	2	50	36	26 ± 3 (n = 3)
5	**[^{18}F]5c**	0.5	4	25	100	51 ± 7 (n = 4)
6	**[^{18}F]5f**	0.05	2	50	73	48 ± 8 (n = 3)
7	**[^{18}F]5f**	0.1	2	50	98	55 ± 1 (n = 3)
8	**[^{18}F]5f**	0.1	2.5	40	100	56 ± 1 (n = 3)

[(a)] Standard reaction conditions for the photoredox C–H ^{18}F-difluoromethylation: substrate **7e** (0.02 mmol), **[^{18}F]5a**, **[^{18}F]5c**, or **[^{18}F]5f** (30–40 MBq), *fac*-Ir^{III}(ppy)$_3$ (mol %), residence time (min), flow rate (μL·min^{-1}), DMSO (250 μL), 35 °C, blue light-emitting diode (LED) (470 nm, 2 W). [(b)] UPLC conversion of the reagents **[^{18}F]5a**, **[^{18}F]5c**, or **[^{18}F]5f**. [(c)] All RCYs were determined based on the radio-TLC and radio-UPLC purities of the crude product **[^{18}F]8e**.

Having identified the optimal conditions for the photoredox C–H ^{18}F-difluoromethylation with **[^{18}F]5a**, **[^{18}F]5c**, and **[^{18}F]5f**, we then investigated the scope of the developed photochemical process (Scheme 5). Gratifyingly, the C–H ^{18}F-difluoromethylation of a series of structurally-diverse heteroarenes such as 4-methyl-1*H*-pyrrolo[2,3-*b*]pyridine (**7a**), 6-methyl-1*H*-pyrazolo[3,4-*b*]pyridine (**7b**), 2-methyl-5,8-dihydropyrido[2,3-*d*]pyrimidin-7(6*H*)-one (**7c**), and ethyl isonicotinate (**7d**) successfully afforded the corresponding products **[^{18}F]8a**–**[^{18}F]8d** in 17–57%, 13–66%, and 14–57% RCYs, using the reagents **[^{18}F]5a**, **[^{18}F]5c**, and **[^{18}F]5f**, respectively. A mixture of structural isomers was observed after the C–H ^{18}F-difluoromethylation of the heteroarenes **7a** (**[^{18}F]8aa** and **[^{18}F]8ab**), **7b** (**[^{18}F]8ba** and **[^{18}F]8bb**), and **7d** (**[^{18}F]8da** and **[^{18}F]8db**). Regardless of the employed ^{18}F-difluoromethylating reagent, the ratio between the distinct isomers was not significantly changed. Besides the antiherpetic drug **7e** [48], the C–H ^{18}F-difluoromethylation procedure was also extended to other heteroarenes of medicinal relevance, in particular to the demethylated derivative of the antihypertensive drug moxonidine (**7f**) [49] and to the xanthine derivative pentoxifylline (**7g**) [50]. The respective [^{18}F]heteroaryl–CF_2H derivatives **[^{18}F]8f** and **[^{18}F]8g** were attained in 21–52%, 17–30%, and 35–60% RCYs from the reagents **[^{18}F]5a**, **[^{18}F]5c**, and **[^{18}F]5f**, respectively. The UPLC radio-chromatogram retention times of the [^{18}F]heteroaryl–CF_2H derivatives **[^{18}F]8a**–**[^{18}F]8g** were in agreement with those of the respective non-radioactive authentic references (Figures S87–S103).

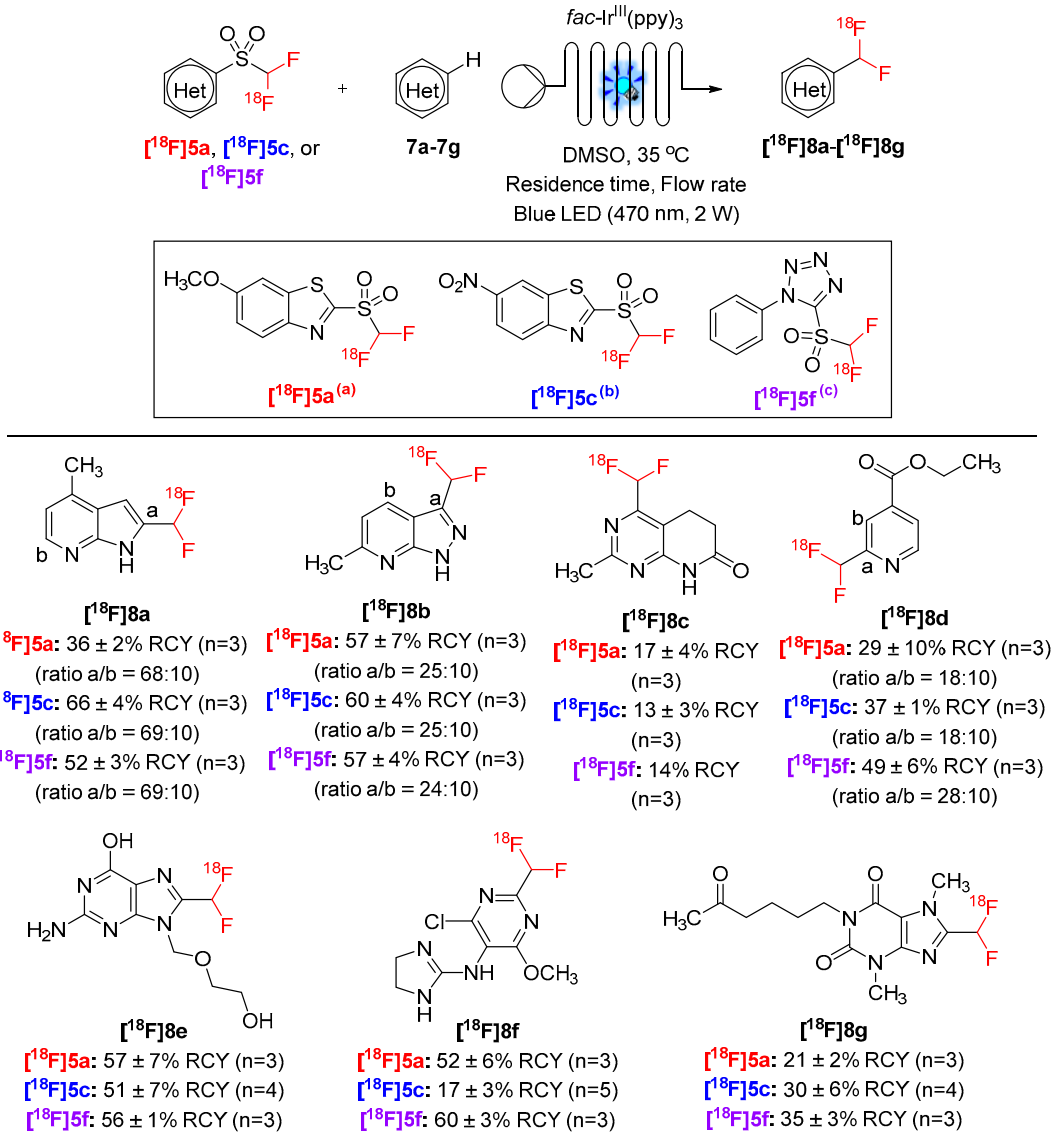

Scheme 5. Scope of [^{18}F]heteroaryl-CF_2H derivatives **[^{18}F]8a–[^{18}F]8g**. Reactions were conducted on a 0.02 mmol scale. [(a)] Conditions: **[^{18}F]5a** (30–40 MBq), *fac*-$Ir^{III}(ppy)_3$ (0.05 mol %), residence time (2 min), flow rate (50 μL·min^{-1}), DMSO (250 μL), 35 °C, blue LED (470 nm, 2 W). [(b)] Conditions: **[^{18}F]5c** (30–40 MBq), *fac*-$Ir^{III}(ppy)_3$ (0.5 mol %), residence time (4 min), flow rate (25 μL·min^{-1}), DMSO (250 μL), 35 °C, blue LED (470 nm, 2 W). [(c)] Conditions: **[^{18}F]5f** (30–40 MBq), *fac*-$Ir^{III}(ppy)_3$ (0.1 mol %), residence time (2.5 min), flow rate (40 μL·min^{-1}), DMSO (250 μL), 35 °C, blue LED (470 nm, 2 W). All RCYs were determined based on the radio-TLC and radio-UPLC purities of the crude products **[^{18}F]8a–[^{18}F]8g**.

To gain insights into the mechanism, the C–H ^{18}F-difluoromethylation of the substrate **7e** was examined. The addition of the radical scavenger 2,2,6,6-tetramethyl-1-piperidinyloxy (TEMPO) to the reaction system completely inhibited the C–H ^{18}F-difluoromethylation of the substrate **7e**, in the presence of the sulfones **[^{18}F]5a**, **[^{18}F]5c**, and **[^{18}F]5f** (Scheme 6, Entry 1). Furthermore, when the model reaction was performed without blue light irradiation (Scheme 6, Entry 2) and photocatalyst (Scheme 6, Entry 3), no desired product **[^{18}F]8e** was formed. These results suggest the involvement of radical intermediates in the present photocatalytic C–H ^{18}F-difluoromethylation reaction. On the basis of these observations and previous research works reporting photoredox C–H difluoromethylation reactions with the sulfones **1** [39–44] and **2** [45], a general and simplified reaction mechanism is shown in Figure 7. The proposed mechanism for the C–H ^{18}F-difluoromethylation of heteroarenes **7a–7g** involved the

reduction of the [^{18}F]difluoromethyl heteroaryl sulfones (**[^{18}F]5a**, **[^{18}F]5c**, and **[^{18}F]5f**), *via* an oxidative quenching of the photoexcited *fac*-Ir^{III}(ppy)$_3$, to generate the [^{18}F]CF$_2$H radicals. The radical C–H ^{18}F-difluoromethylation of the substrates **7a–7g** in favourable reaction site(s) would result in the formation of [^{18}F]heteroaryl-CF$_2$H radical intermediates. Subsequent oxidation by *fac*-Ir^{IV}(ppy)$_3$ and deprotonation would afford the corresponding [^{18}F]heteroaryl–CF$_2$H derivatives **[^{18}F]8a–[^{18}F]8g**.

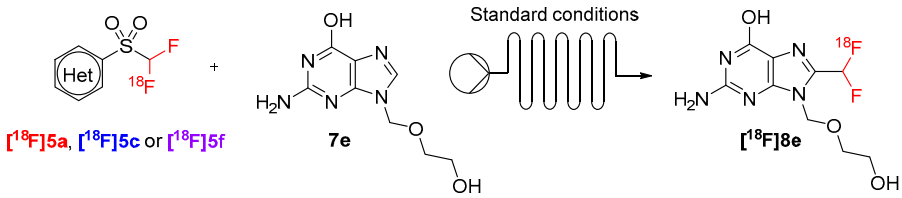

Entry	Deviation to the standard conditions	RCY (%)
1	TEMPO (0.02 mmol)	0
2	No blue LED irradiation	0
3	No catalyst	0

Scheme 6. Control experiments with the radical scavenger 2,2,6,6-tetramethyl-1-piperidinyloxy (TEMPO) (Entry 1), in the absence of blue light irradiation (Entry 2), and in the absence of photocatalyst (Entry 3). Reactions were conducted on a 0.02 mmol scale. Standard conditions: (i) **[^{18}F]5a** (30–40 MBq), *fac*-Ir^{III}(ppy)$_3$ (0.05 mol %), residence time (2 min), flow rate (50 µL·min^{-1}), DMSO (250 µL), 35 °C, blue LED (470 nm, 2 W); (ii) **[^{18}F]5c** (30–40 MBq), *fac*-Ir^{III}(ppy)$_3$ (0.5 mol %), residence time (4 min), flow rate (25 µL·min^{-1}), DMSO (250 µL), 35 °C, blue LED (470 nm, 2 W); (iii) **[^{18}F]5f** (30–40 MBq), *fac*-Ir^{III}(ppy)$_3$ (0.1 mol %), residence time (2.5 min), flow rate (40 µL·min^{-1}), DMSO (250 µL), 35 °C, blue LED (470 nm, 2 W).

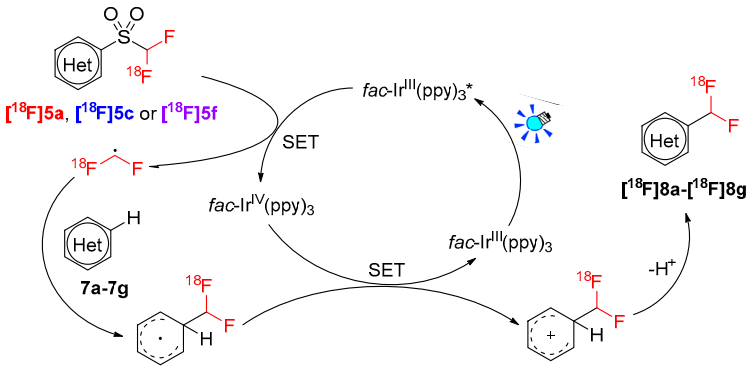

Figure 7. A general and simplified mechanism for the C–H ^{18}F-difluoromethylation of **7a–7g** with the sulfones **[^{18}F]5a**, **[^{18}F]5c**, and **[^{18}F]5f**.

3. Materials and Methods

3.1. Chemistry

All solvents and reagents were purchased from Sigma Aldrich (Overijse, Belgium), TCI Europe N.V. (Zwijndrecht, Belgium), abcr GmbH (Karlsruhe, Germany), or VWR (Oud-Heverlee, Belgium), and no further purification process was implemented. Solvents were evaporated using a HEI-VAP rotary evaporator (Heidolph, Germany). Thin-layer chromatography (TLC) analyses were carried out on silica gel Polygram® SIL G/UV$_{254}$ pre-coated TLC-sheets (Macherey-Nagel, Düren, Germany). Ultra-performance liquid chromatography (UPLC) analyses were carried out on a Waters system (ACQUITY UPLC® PDA UV detector (190–400 nm), Waters, Milford, MA, USA) controlled by the Empower software and with an ACQUITY UPLC® CSH C18 column (1.7 µm, 2.1 × 100 mm) (Waters, Milford, MA, USA), at 0.5 mL·min^{-1} and 45 °C. Purifications by flash chromatography

were carried out automatically by a CombiFlash® system (Teledyne Isco, San Diego, CA, USA) with RediSep® Rf Normal Phase Silica columns (sizes: 24 g, 40 g, and 80 g). ^{1}H-, ^{13}C-, and ^{19}F-nuclear magnetic resonance (NMR) spectra were recorded at room temperature on a Bruker AVANCE III UltraShield NanoBay 400 MHz NMR Spectrometer (400 MHz for ^{1}H, 101 MHz for ^{13}C, and 376 MHz for ^{19}F, Bruker Biosciences Corporation, Billerica, MA, USA). The newly synthesized compounds were analyzed in DMSO-d^6 and $CDCl_3$ at a probe temperature of 300 K. For ^{1}H- and ^{13}C-NMR spectra, the chemical shifts (δ) were expressed in ppm downfield from tetramethylsilane (TMS) as an internal standard. For ^{19}F-NMR spectra, the chemical shifts (δ) were given in ppm downfield from trifluoroacetic acid (TFA, δ = −76.50 ppm) as internal standard. The NMR multiplicity signals were abbreviated as: s = singlet, d = doublet, t = triplet, dd = doublet of doublets, ddd = doublet of doublet of doublets, or m = multiplet. The coupling constants (J) were given in Hz and reported to the nearest 1 Hz. High-resolution mass spectroscopy (HRMS) spectra were measured on using a SYNAPT G2-SI Waters Q-TOF mass spectrometer (Waters, Milford, MA, USA). This spectrometer is equipped with an electrospray ionization (ESI) source and a Waters Acquity H-class UPLC with diode array detector (210 to 400 nm) (Waters, Milford, MA, USA). An Acquity UPLC HSS T3 C18 column (1.8 µm, 2.1 × 50 mm) was used. The melting points (m.p.) of the solid compounds were measured using a Büchi® melting point apparatus (model B-545, AC/DC input 230 V AC, Büchi, Flawil, Switzerland).

3.1.1. General Procedure for the Synthesis of Difluoromethyl Heteroaryl-Sulfides (**4a**–**4f**)

The difluoromethylation of heteroaryl-thiols (**3a**–**3f**) was achieved following the slightly modified protocols [46,47]. Sodium chlorodifluoroacetate (915 mg, 6.0 mmol, 2.0 equiv.) and potassium carbonate (622 mg, 4.5 mmol, 1.5 equiv.) were added to a single-neck round-bottom flask with DMF (5 mL) and the resulting suspension was stirred at room temperature for 5 minutes. Afterwards, a solution of the heteroaryl-thiols **3a**–**3f** (3.0 mmol, 1.0 equiv.) in DMF (5 mL) was slowly added. The reaction mixture was stirred at 95 °C for 15 minutes and then cooled down to room temperature. After dilution with H_2O (10 mL), the crude product was extracted with DCM (3 × 20 mL). The organic layers were gathered and dried over anhydrous $MgSO_4$. After filtration, the solution was concentrated under reduced pressure and the resulting crude product was purified by flash chromatography as described below.

2-((Difluoromethyl)thio)-6-methoxybenzo[d]thiazole (**4a**). Purified by flash chromatography (SiO_2; heptane/EtOAc (95/5, *v*/*v*)). Yellow oil (363 mg, 49% yield); ^{1}H-NMR (DMSO-d^6, 400 MHz): δ = 7.95 (1H, dd, J_{HH} = 9.0 and 0.4 Hz), 7.87 (1H, t, J_{HF} = 54.9 Hz), 7.73 (1H, d, J_{HH} = 2.6 Hz), 7.17 (1H, dd, J_{HH} = 9.0 and 2.6 Hz), 3.84 (3H, s) ppm; ^{13}C-NMR (DMSO-d^6, 101 MHz): δ = 157.8, 151.6 (t, J_{CF} = 3.9 Hz), 147.0, 138.1, 123.3, 120.3 (t, J_{CF} = 276.1 Hz), 116.3, 104.5, 55.8 ppm; ^{19}F-NMR (DMSO-d^6 + TFA, 376 MHz): δ = −95.8 (2F, d, J_{HF} = 54.9 Hz) ppm; *m*/*z* $[C_9H_7F_2NOS_2 + H]^+$ calcd. for $[C_9H_8F_2NOS_2]$: 248.0015; found: 248.0018.

2-((Difluoromethyl)thio)-5-methoxybenzo[d]thiazole (**4b**). Purified by flash chromatography (SiO_2; heptane/EtOAc (95/5, *v*/*v*)). White powder (317 mg, 43% yield); m.p. 48-49 °C; ^{1}H-NMR (DMSO-d^6, 400 MHz): δ = 8.01 (1H, dd, J_{HH} = 8.9 and 0.3 Hz), 7.93 (1H, t, J_{HF} = 54.8 Hz), 7.59 (1H, d, J_{HH} = 2.4 Hz), 7.15 (1H, dd, J_{HH} = 9.0 and 2.4 Hz), 3.85 (3H, s) ppm; ^{13}C-NMR (DMSO-d^6, 101 MHz): δ = 158.9, 156.5 (t, J_{CF} = 3.7 Hz), 153.8, 127.8, 122.4, 120.3 (t, J_{CF} = 275.7 Hz), 115.8, 105.2, 55.6 ppm; ^{19}F-NMR (DMSO-d^6 + TFA, 376 MHz): δ = −96.1 (2F, d, J_{HF} = 54.5 Hz) ppm; *m*/*z* $[C_9H_7F_2NOS_2 + H]^+$ calcd. for $[C_9H_8F_2NOS_2]$: 248.0015; found: 248.0025.

2-((Difluoromethyl)thio)-6-nitrobenzo[d]thiazole (**4c**). Purified by flash chromatography (SiO_2; heptane/DCM (60/40, *v*/*v*)). Light yellow powder (139 mg, 18% yield); m.p. 96–97 °C; ^{1}H-NMR (DMSO-d^6, 400 MHz): δ = 9.18 (1H, d, J_{HH} = 2.4 Hz), 8.34 (1H, dd, J_{HH} = 9.0 and 2.4 Hz), 8.18 (1H, d, J_{HH} = 9.0 Hz), 8.06 (1H, t, J_{HF} = 54.4 Hz) ppm; ^{13}C-NMR (DMSO-d^6, 101 MHz): δ = 164.6 (t, J_{CF} = 3.7 Hz), 155.6, 144.5, 136.2, 122.6, 122.1, 120.2 (t, J_{CF} = 276.2 Hz), 119.2 ppm; ^{19}F-NMR (DMSO-d^6 + TFA, 376 MHz): δ = −95.2 (2F, d, J_{HF} = 54.4 Hz) ppm; *m*/*z* $[C_8H_4F_2N_2O_2S_2 + H]^+$ calcd. for $[C_8H_5F_2N_2O_2S_2]$: 262.976; found: 262.976.

2-((Difluoromethyl)thio)-5-nitrobenzo[d]thiazole (**4d**). Purified by flash chromatography (SiO_2; heptane/DCM (60/40, *v*/*v*)). Light yellow powder (155 mg, 20% yield); m.p. 79–80 °C; ^{1}H-NMR (DMSO-d^6, 400 MHz): δ = 8.77 (1H, d, J_{HH} = 2.2 Hz), 8.42 (1H, d, J_{HH} = 8.9 Hz), 8.32 (1H, dd, J_{HH} = 8.9 and 2.3 Hz), 8.03 (1H, t, J_{HF} = 54.4 Hz) ppm; ^{13}C-NMR (DMSO-d^6, 101 MHz): δ = 161.7 (t, J_{CF} = 3.6 Hz), 151.7, 146.7, 142.5, 123.5, 120.2 (t, J_{CF} = 276.2 Hz), 119.9, 117.2 ppm; ^{19}F-NMR (DMSO-d^6 + TFA, 376 MHz): δ = −94.8 (2F, d, J_{HF} = 54.4 Hz) ppm; *m*/*z* [$C_8H_4F_2N_2O_2S_2$ + H]$^+$ calcd. for [$C_8H_5F_2N_2O_2S_2$]: 262.976; found: 262.976.

2-((Difluoromethyl)thio)-1-methyl-1H-benzo[d]imidazole (**4e**). Purified by flash chromatography (SiO_2; heptane/EtOAc (95/5, *v*/*v*)). Light yellow powder (333 mg, 52% yield); m.p. 44–45 °C; ^{1}H-NMR (DMSO-d^6, 400 MHz): δ = 7.78 (1H, t, J_{HF} = 55.4 Hz), 7.69–7.67 (1H, m), 7.63–7.61 (1H, m), 7.35–7.32 (1H, m), 7.29–7.25 (1H, m), 3.83 (3H, s) ppm; ^{13}C-NMR (DMSO-d^6, 101 MHz): δ = 142.7, 141.7 (t, J_{CF} = 4.7 Hz), 136.3, 123.2, 122.4, 120.9 (t, J_{CF} = 275.1 Hz), 118.9, 110.7, 30.8 ppm; ^{19}F-NMR (DMSO-d^6 + TFA, 376 MHz): δ = −93.6 (2F, d, J_{HF} = 55.4 Hz) ppm; *m*/*z* [$C_9H_8F_2N_2S$ + H]$^+$ calcd. for [$C_9H_9F_2N_2S$]: 215.0455; found: 215.0455.

5-((Difluoromethyl)thio)-1-phenyl-1H-tetrazole (**4f**). Purified by flash chromatography (SiO_2; heptane/EtOAc (95/5, *v*/*v*)). Yellow oil (395 mg, 58% yield); ^{1}H-NMR ($CDCl_3$, 400 MHz): δ = 7.73 (1H, t, J_{HF} = 55.9 Hz), 7.63–7.60 (3H, m), 7.53–7.50 (2H, m) ppm; ^{13}C-NMR ($CDCl_3$, 101 MHz): δ = 148.3 (t, J_{CF} = 5.0 Hz), 132.9, 131.1, 130.2, 124.3, 119.5 (t, J_{CF} = 279.8 Hz) ppm; ^{19}F-NMR ($CDCl_3$ + TFA, 376 MHz): δ = −92.6 (2F, d, J_{HF} = 55.4 Hz) ppm; *m*/*z* [$C_8H_6F_2N_4S$ + H]$^+$ calcd. for [$C_8H_7F_2N_4S$]: 229.0359; found: 229.0362.

3.1.2. General Procedure for the Synthesis of Difluoromethyl Heteroaryl-Sulfones (**5a**–**5f**)

To a round-bottom flask containing the difluoromethyl heteroaryl-sulfides **4a**–**4f** (1.0 mmol, 1.0 equiv.) in MeCN (2 mL) and $CHCl_3$ (2 mL), a solution of sodium (meta)periodate ($NaIO_4$) (1.07 g, 5.0 mmol, 5 equiv.) and ruthenium (III) chloride hydrate ($RuCl_3{\cdot}xH_2O$) (10 mg, 0.05 mmol, 0.05 equiv.) in H_2O (4 mL) was added to the reaction system. The resulting reaction mixture was stirred at room temperature for 1 h. After the completion of the reaction, the suspension was diluted with H_2O (5 mL) and the crude product was extracted with DCM (3 × 25 mL). The combined organic layers were washed with saturated aqueous solution of $NaHCO_3$ and subsequently dried over anhydrous $MgSO_4$. After filtration, the solvent was evaporated under reduced pressure. The resulting crude product was then purified by flash chromatography (SiO_2; heptane/EtOAc (90/10, *v*/*v*)) to afford the difluoromethyl heteroaryl-sulfones 5a–5f as pure compounds.

2-((Difluoromethyl)sulfonyl)-6-methoxybenzo[d]thiazole (**5a**). Light yellow powder (121 mg, 87% yield); m.p. 129-130 °C; ^{1}H-NMR (DMSO-d^6, 400 MHz): δ = 8.27 (1H, d, J_{HH} = 9.2 Hz), 7.96 (1H, d, J_{HH} = 2.6 Hz), 7.65 (1H, t, J_{HF} = 51.6 Hz), 7.38 (1H, dd, J_{HH} = 9.2 and 2.6 Hz), 3.91 (3H, s) ppm; ^{13}C-NMR (DMSO-d^6, 101 MHz): δ = 160.1, 155.0, 147.1, 140.0, 126.4, 119.4, 114.9 (t, J_{CF} = 284.9 Hz), 104.8, 56.1 ppm; ^{19}F-NMR (DMSO-d^6 + TFA, 376 MHz): δ = −126.0 (2F, d, J_{HF} = 51.7 Hz) ppm; *m*/*z* [$C_9H_7F_2NO_3S_2$ + H]$^+$ calcd. for [$C_9H_8F_2NO_3S_2$]: 279.9914; found: 279.9915.

2-((Difluoromethyl)sulfonyl)-5-methoxybenzo[d]thiazole (**5b**). Yellow powder (89 mg, 64% yield); m.p. 110-111 °C; ^{1}H-NMR (DMSO-d^6, 400 MHz): δ = 8.29 (1H, d, J_{HH} = 9.1 Hz), 7.90 (1H, d, J_{HH} = 2.4 Hz), 7.67 (1H, t, J_{HF} = 51.5 Hz), 7.43 (1H, dd, J_{HH} = 9.2 and 2.5 Hz), 3.91 (3H, s) ppm; ^{13}C-NMR (DMSO-d^6, 101 MHz): δ = 160.0, 159.2, 154.1, 129.9, 124.1, 120.4, 115.0 (t, J_{CF} = 285.4 Hz), 106.6, 55.9 ppm; ^{19}F-NMR (DMSO-d^6 + TFA, 376 MHz): δ = −125.9 (2F, d, J_{HF} = 51.7 Hz) ppm; *m*/*z* [$C_9H_7F_2NO_3S_2$ + H]$^+$ calcd. for [$C_9H_8F_2NO_3S_2$]: 279.9914; found: 279.9917.

2-((Difluoromethyl)sulfonyl)-6-nitrobenzo[d]thiazole (**5c**). Light yellow powder (115 mg, 78% yield); m.p. 161–162 °C; ^{1}H-NMR (DMSO-d^6, 400 MHz): δ = 9.46 (1H, d, J_{HH} = 2.4 Hz), 8.62 (1H, d, J_{HH} = 9.1 Hz), 8.54 (1H, dd, J_{HH} = 9.2 and 2.4 Hz), 7.76 (1H, t, J_{HF} = 51.4 Hz) ppm; ^{13}C-NMR (DMSO-d^6, 101 MHz): δ = 165.0, 155.4, 146.6, 137.9, 126.5, 123.3, 121.1, 115.1 (t, J_{CF} = 285.5 Hz) ppm; ^{19}F-NMR (DMSO-d^6

+ TFA, 376 MHz): δ = −123.9 (2F, d, J_{HF} = 51.5 Hz) ppm; *m/z* [$C_8H_4F_2N_2O_4S_2$ + H]$^+$ calcd. for [$C_8H_5F_2N_2O_4S_2$]: 294.9659; found: 294.9671.

2-((Difluoromethyl)sulfonyl)-5-nitrobenzo[d]thiazole (**5d**). White powder (120 mg, 82% yield); m.p. 168–169 °C; ^{1}H-NMR (DMSO-d^6, 400 MHz): δ = 9.23 (1H, dd, J_{HH} = 2.2 and 0.4 Hz), 8.70 (1H, dd, J_{HH} = 9.1 and 0.4 Hz), 8.57 (1H, dd, J_{HH} = 9.1 and 2.2 Hz), 7.74 (1H, t, J_{HF} = 51.3 Hz) ppm; ^{13}C-NMR (DMSO-d^6, 101 MHz): δ = 163.3, 151.8, 147.7, 143.4, 125.5, 122.9, 121.0, 115.1 (t, J_{CF} = 286.0 Hz) ppm; ^{19}F-NMR (DMSO-d^6 + TFA, 376 MHz): δ = −123.9 (2F, d, J_{HF} = 51.4 Hz) ppm; *m/z* [$C_8H_4F_2N_2O_4S_2$ + H]$^+$ calcd. for [$C_8H_5F_2N_2O_4S_2$]: 294.9659; found: 294.966.

2-((Difluoromethyl)sulfonyl)-1-methyl-1H-benzo[d]imidazole (**5e**). White powder (82 mg, 67% yield); m.p. 134–135 °C; ^{1}H-NMR (DMSO-d^6, 400 MHz): δ = 7.94–7.92 (1H, m), 7.88–7.86 (1H, m), 7.61 (1H, t, J_{HF} = 51.9 Hz), 7.62–7.58 (1H, m), 7.50–7.46 (1H, m), 4.14 (3H, s) ppm; ^{13}C-NMR (DMSO-d^6, 101 MHz): δ = 141.1, 140.9, 136.7, 127.0, 124.7, 121.4, 114.8 (t, J_{CF} = 283.9 Hz), 112.4, 32.1 (t, J_{CF} = 0.8 Hz) ppm; ^{19}F-NMR (DMSO-d^6 + TFA, 376 MHz): δ = −125.6 (2F, d, J_{HF} = 51.9 Hz) ppm; *m/z* [$C_9H_8F_2N_2O_2S$ + H]$^+$ calcd. for [$C_9H_9F_2N_2O_2S$]: 247.0352; found: 247.0353.

5-((Difluoromethyl)sulfonyl)-1-phenyl-1H-tetrazole (**5f**). White powder (85 mg, 65% yield); m.p. 68–69 °C; ^{1}H-NMR ($CDCl_3$, 400 MHz): δ = 7.72–7.59 (5H, m), 6.83 (1H, t, J_{HF} = 52.9 Hz) ppm; ^{13}C-NMR ($CDCl_3$, 101 MHz): δ = 132.5, 132.2, 130.1, 125.4, 114.2 (t, J_{CF} = 289.3 Hz), 104.9 ppm; ^{19}F-NMR ($CDCl_3$ + TFA, 376 MHz): δ = −124.1 (2F, d, J_{HF} = 52.9 Hz) ppm; *m/z* [$C_8H_6F_2N_4O_2S$ + H]$^+$ calcd. for [$C_8H_7F_2N_4O_2S$]: 261.0258; found: 261.0257.

3.1.3. General Procedure for the Synthesis of Bromofluoromethyl Heteroaryl-Sulfides (**6a**–**6f**)

The bromofluoromethylation of heteroaryl-thiols (**3a**–**3f**) was carried out on the basis of a previously described procedure [37] with slight modifications. A solution of KOH (1.68 g, 30.0 mmol, 10.0 equiv.) in H_2O (4 mL) was placed in a single-neck round-bottom flask and stirred at 0°C. Afterwards, a solution of the heteroaryl-thiols **3a**–**3f** (3.0 mmol, 1.0 equiv.) in THF (3 mL) was added and the resulting mixture was allowed to stir at room temperature for 20 min. A solution of dibromofluoromethane (0.713 mL, 9.0 mmol, 3.0 equiv.) in THF (1 mL) was slowly introduced in the reaction system, and the resulting mixture was stirred at room temperature for 15–20 min. The suspension was subsequently quenched by addition of H_2O (20 mL), and the crude product was extracted with DCM (3 × 30 mL). The combined organic layers were gathered and were dried over anhydrous $MgSO_4$. After filtration, the solvent was removed under reduced pressure. The purification of the concentrated crude product was performed by flash chromatography (SiO_2; heptane/EtOAc (95/5, *v/v*)) to furnish the bromofluoromethyl heteroaryl-sulfides **6a**–**6f** as pure compounds.

2-((Bromofluoromethyl)thio)-6-methoxybenzo[d]thiazole (**6a**). Yellow powder (182 mg, 20% yield); m.p. 53-55 °C; ^{1}H-NMR (DMSO-d^6, 400 MHz): δ = 8.35 (1H, d, J_{HF} = 53.7 Hz), 7.94 (1H, d, J_{HH} = 9.0 Hz), 7.73 (1H, d, J_{HH} = 2.6 Hz), 7.16 (1H, dd, J_{HH} = 9.0 and 2.6 Hz), 3.84 (3H, s) ppm; ^{13}C-NMR (DMSO-d^6, 101 MHz): δ = 157.8, 155.3 (d, J_{CF} = 2.8 Hz), 146.8, 137.9, 123.3, 116.4, 104.6, 91.2 (d, J_{CF} = 294.5 Hz), 55.8 ppm; ^{19}F-NMR (DMSO-d^6 + TFA, 376 MHz): δ = −105.0 (1F, d, J_{HF} = 53.8 Hz) ppm; *m/z* [$C_9H_7BrFNOS_2$ + H]$^+$ calcd. for [$C_9H_8BrFNOS_2$]: 307.9214; found: 307.9218.

2-((Bromofluoromethyl)thio)-5-methoxybenzo[d]thiazole (**6b**). Yellow oil (166 mg, 18% yield); ^{1}H-NMR (DMSO-d^6, 400 MHz): δ = 8.39 (1H, d, J_{HF} = 53.8 Hz), 8.01 (1H, d, J_{HH} = 9.0 Hz), 7.58 (1H, d, J_{HH} = 2.5 Hz), 7.14 (1H, dd, J_{HH} = 9.0 and 2.5 Hz), 3.85 (3H, s) ppm; ^{13}C-NMR (DMSO-d^6, 101 MHz): δ = 160.1 (d, J_{CF} = 2.8 Hz), 159.0, 153.6, 127.7, 122.5, 115.8, 105.3, 90.8 (d, J_{CF} = 293.3 Hz), 55.6 ppm; ^{19}F-NMR (DMSO-d^6 + TFA, 376 MHz): δ = −105.6 (1F, d, J_{HF} = 54.1 Hz) ppm; *m/z* [$C_9H_7BrFNOS_2$ + H]$^+$ calcd. for [$C_9H_8BrFNOS_2$]: 307.9214; found: 307.9223.

2-((Bromofluoromethyl)thio)-6-nitrobenzo[d]thiazole (**6c**). Light yellow powder (105 mg, 11% yield); m.p. 115–117 °C; ^{1}H-NMR (DMSO-d^6, 400 MHz): δ = 9.20 (1H, dd, J_{HH} = 2.4 and 0.4 Hz), 8.53 (1H, d, J_{HF}

= 53.8 Hz), 8.35 (1H, dd, J_{HH} = 9.0 and 2.4 Hz), 8.17 (1H, dd, J_{HH} = 9.0 and 0.4 Hz) ppm; ^{13}C-NMR (DMSO-d^6, 101 MHz): δ = 167.9 (d, J_{CF} = 3.0 Hz), 155.6, 144.4, 136.2, 122.6, 122.1, 119.4, 90.1 (d, J_{CF} = 293.5 Hz) ppm; ^{19}F-NMR (DMSO-d^6 + TFA, 376 MHz): δ = −107.5 (1F, d, J_{HF} = 54.1 Hz) ppm; *m/z* [$C_8H_4BrFN_2O_2S_2$ + H]$^+$ calcd. for [$C_8H_5BrFN_2O_2S_2$]: 322.896; found: 322.8952.

2-((Bromofluoromethyl)thio)-5-nitrobenzo[d]thiazole (**6d**). Orange powder (88 mg, 9% yield); m.p. 93–95 °C; ^{1}H-NMR (DMSO-d^6, 400 MHz): δ = 8.76 (1H, d, J_{HH} = 2.2 Hz), 8.50 (1H, d, J_{HF} = 53.6 Hz), 8.43 (1H, d, J_{HH} = 9.0 Hz), 8.31 (1H, dd, J_{HH} = 9.0 and 2.2 Hz) ppm; ^{13}C-NMR (DMSO-d^6, 101 MHz): δ = 165.1 (d, J_{CF} = 2.9 Hz), 151.6, 146.7, 142.4, 123.6, 119.9, 117.2, 90.3 (d, J_{CF} = 293.4 Hz) ppm; ^{19}F-NMR (DMSO-d^6 + TFA, 376 MHz): δ = −106.7 (1F, d, J_{HF} = 53.6 Hz) ppm; *m/z* [$C_8H_4BrFN_2O_2S_2$ + H]$^+$ calcd. for [$C_8H_5BrFN_2O_2S_2$]: 322.896; found: 322.8964.

2-((Bromofluoromethyl)thio)-1-methyl-1H-benzo[d]imidazole (**6e**). Light yellow powder (214 mg, 26% yield); m.p. 79–80 °C; ^{1}H-NMR (DMSO-d^6, 400 MHz): δ = 8.19 (1H, d, J_{HF} = 54.0 Hz), 7.70-7.68 (1H, m), 7.64–7.62 (1H, m), 7.36–7.32 (1H, m), 7.30–7.26 (1H, m), 3.83 (3H, s) ppm; ^{13}C-NMR (DMSO-d^6, 101 MHz): δ = 144.7 (d, J_{CF} = 1.8 Hz), 142.4, 136.1, 123.4, 122.5, 118.9, 110.9, 91.5 (d, J_{CF} = 294.9 Hz), 30.8 ppm; ^{19}F-NMR (DMSO-d^6 + TFA, 376 MHz): δ = −104.6 (2F, d, J_{HF} = 53.8 Hz). HRMS (ESI$^+$) ppm; *m/z* [$C_9H_8BrFN_2S$ + H]$^+$ calcd. for [$C_9H_9BrFN_2S$]: 274.9654; found: 274.9662.

5-((Bromofluoromethyl)thio)-1-phenyl-1H-tetrazole (**6f**). Yellow oil (171 mg, 20% yield); ^{1}H-NMR (DMSO-d^6, 400 MHz): δ = 8.16 (1H, d, J_{HF} = 52.8 Hz), 7.72–7.67 (5H, m) ppm; ^{13}C-NMR (DMSO-d^6, 101 MHz): 149.7 (d, J_{CF} = 3.0 Hz), 132.9, 131.0, 129.9, 125.4, 89.9 (d, J_{CF} = 295.9 Hz) ppm; ^{19}F-NMR (DMSO-d^6 + TFA, 376 MHz): δ = −105.3 (1F, d, J_{HF} = 53.0 Hz) ppm; *m/z* [C_6H_5BrFN + H]$^+$ calcd. for [C_6H_6BrFN]: 288.9559; found: 288.9563.

3.1.4. General Procedure for the Synthesis of the Difluoromethylated Heteroarenes (**8a**–**8g**)

The difluoromethylated heteroarenes **8a**–**8g** were synthesized from the heteroarenes **7a**–**7g** and characterized according to the formerly reported procedures [37,51].

3.2. Radiochemistry

Semi-preparative high performance liquid chromatography (HPLC) purification was conducted on a XBridge® BEH C18 OBD™ Prep column (130 Å, 5 µm, 10 mm × 250 mm; Waters, Milford, MA, USA) with a mixture of MeCN/H_2O (40/60, *v/v*) in isocratic mode (flow rate: 5 mL·min^{-1}). The radio-HPLC profiles were monitored with a custom homemade Geiger-Muller (GM) radioactivity detector (Thermo Fisher Scientific, Waltham, MA, USA), connected to the semi-preparative HPLC system. Ultra performance liquid chromatography (UPLC) analyses were performed at 45 °C using an ACQUITY UPLC® CSH™ C18 column (2.1 × 100 mm, 1.7 µm; Waters, Milford, MA, USA) on an ACQUITY UPLC® system with a mobile phase of MeCN and HCO_2H/H_2O (0.05%, *v/v*) in gradient mode at 0.5 mL·min^{-1} (gradient A: from 100% HCO_2H/H_2O (0.05%, *v/v*) to 75% MeCN + 25% HCO_2H/H_2O (0.05%, *v/v*) in 6 min, and from 75% MeCN + 25% HCO_2H/H_2O (0.05%, *v/v*) to 100% H_2O in 2 min; gradient B: from 100% HCO_2H/H_2O (0.05%, *v/v*) to 100% MeCN in 6 min, and from 100% MeCN to 100% HCO_2H/H_2O (0.05%, *v/v*) in 2 min). The UV signal of the newly synthesized ^{18}F-labeled compounds was measured at 254 nm with a photodiode array (PDA) UV detector (190–400 nm) controlled by the Empower software and connected to the UPLC system. A thallium-activated sodium iodide (NaI(Tl)) scintillation detector from Eberline (Eberline Instruments Corp, Miami, FL, USA) was used to monitor the radio-UPLC elution profile of the newly synthesized ^{18}F-labeled compounds. TLC analyses were carried out on silica gel Polygram® SIL G/UV_{254} pre-coated TLC-sheets (TLC eluent: methanol) (Macherey-Nagel, Düren, Germany). The TLC profile of ^{18}F-labeled compounds was then analyzed with a BertHold TLC scanner model AR2000 (BertHold, Bad Wildbad, Germany).

The radiosyntheses of the ^{18}F-labeled compounds was achieved using the commercially available FASTlab™ synthesizer (GE Healthcare, Chicago, IL, USA). The SepPak® cartridges (SepPak® AccellTM Plus QMA Carbonate Plus Light Cartridge (46 mg, 40 µm) and SepPak® ^{t}C18 Plus Short Cartridge

(400 mg, 37–55 μm) were purchased from Waters (Milford, MA, USA). No-carrier-added [^{18}F]fluoride was prepared from the ^{18}O-enriched water ([^{18}O]H_2O) *via* the ^{18}O(p,n)^{18}F nuclear reaction with a Cyclone 18/9 from IBA (Louvain-la-Neuve, Belgium). [^{18}O]H_2O was purchased from Cambridge Isotope Laboratories (Tewksbury, MA, USA). At the end of bombardment (EOB), the activity was transferred to the hot lab cell with helium pressure through Teflon tubing (~50 m).

3.2.1. Fully Automated Radiosyntheses of 2-[^{18}F]((Difluoromethyl)Sulfonyl)-6-Methoxybenzo[*d*]thiazole (**[^{18}F]5a**), 2-[^{18}F]((Difluoromethyl)sulfonyl)-6-nitrobenzo[*d*]thiazole (**[^{18}F]5c**), and 5-[^{18}F]((Difluoromethyl)Sulfonyl)-1-Phenyl-1*H*-Tetrazole (**[^{18}F]5f**)

The fully automated radiosyntheses of the labeled compounds **[^{18}F]5a**, **[^{18}F]5c**, and **[^{18}F]5f** were conducted in a FASTlab^{TM} synthesizer (GE Healthcare, Chicago, IL, USA) according to a radiochemical process previously reported in the literature [37,52]. The reagents and solvents used in the radiosyntheses of **[^{18}F]5a**, **[^{18}F]5c**, and **[^{18}F]5f** were placed in 11 mm- and 13 mm-sealed vials and positioned in the FASTlab^{TM} manifold as depicted in Table S23 and illustrated in Figure 3.

The no-carrier-added (n.c.a.) [^{18}F]fluoride in [^{18}O]H_2O was transferred from the cyclotron target onto the FASTlab^{TM} synthesizer *via* the [^{18}F]fluoride inlet conical reservoir (V6). The [^{18}F]fluoride was trapped on an ion-exchange resin (Sep-Pak® Accell^{TM} Plus QMA Carbonate Plus Light Cartridge; Waters, Milford, MA, USA; from V5 to V4) and the [^{18}O]H_2O was recovered in a separate vial (V1). The trapped [^{18}F]fluoride was eluted into the cyclic olefin copolymer (COC) reactor through a central tubing (V8) with a solution of Kryptofix® 222 ($K_{2.2.2}$; 7.5 mg in 600 μL of MeCN) and K_2CO_3 (1.4 mg in 150 μL of H_2O). The eluent was azeotropically evaporated under vacuum and nitrogen flow by heating at 105 °C and 120 °C for 8 min. Subsequently, a solution of the precursors 6a (12.3 mg, 0.04 mmol), 6c (6.5 mg, 0.02 mmol), or 6f (11.6 mg, 0.04 mmol) solubilized in MeCN (1.0 mL) was transferred to the dry [^{18}F]potassium fluoride/Kryptofix® 222 ([^{18}F]KF/$K_{2.2.2}$) complex *via* the central tubing of the reactor (V8) and heated to 120 °C for 5 min. After the ^{18}F-labeling of **6a**, **6c**, or **6f**, the reaction mixture containing the **[^{18}F]4a**, **[^{18}F]4c**, or **[^{18}F]4f**, respectively, was diluted two times with H_2O (~12 mL) (V15), and the labeled compounds **[^{18}F]4a**, **[^{18}F]4c**, or **[^{18}F]4f** were trapped on a ^{t}C18 cartridge (Sep-Pak® C18 Plus Short Cartridge; Waters, Milford, MA, USA; from V17 to V18). The COC reactor was subsequently washed with H_2O (~4 mL), and the crude solution was passed through the ^{t}C18 cartridge. A solution containing $NaIO_4$ (153.9 mg, 0.072 mmol) and $RuCl_3{\cdot}xH_2O$ (3.4 mg, 0.016 mmol) in H_2O (4.0 mL) was transferred to the ^{t}C18 cartridge and the oxidation of the labeled compounds **[^{18}F]4a**, **[^{18}F]4c**, or **[^{18}F]4f** was carried out on the solid-phase for 5 min at room temperature. Afterwards, the crude products **[^{18}F]5a**, **[^{18}F]5c**, or **[^{18}F]5f** were eluted (from V18 to V17; reverse flow elution) with MeCN (2 mL; syringe S3, V24) and recovered into the reactor through its central tubing. After dilution with H_2O (~4 mL) using the syringe S2 (V11), the resulting mixture was conducted to the semi-preparative HPLC loop (V9; 6 mL) *via* a Sterifix® Paed filter (B. Braun, Melsungen, Germany; 0.2 μm). The COC reactor was subsequently washed with H_2O (~2 mL) and this solution was also transferred into the HPLC loop. The semi-preparative HPLC purification of **[^{18}F]5a**, **[^{18}F]5c**, or **[^{18}F]5f** was accomplished with a mixture of MeCN/H_2O (40/60, *v*/*v*) in isocratic mode at 5 mL·min^{-1}. The HPLC peaks corresponding to the **[^{18}F]5a**, **[^{18}F]5c**, or **[^{18}F]5f** were collected (retention time of **[^{18}F]5a**: 22–26 min; retention time of **[^{18}F]5c**: 19–23 min; retention time of **[^{18}F]5f**: 15–18 min) in a sealed vial containing H_2O (~30 mL). Subsequently, the purified compounds **[^{18}F]5a**, **[^{18}F]5c**, or **[^{18}F]5f** were pumped (from V10), 6 mL by 6 mL, with the syringe S2 (V11) and further conducted to a preconditioned ^{t}C18 cartridge (from V21 to V22). Finally, **[^{18}F]5a**, **[^{18}F]5c**, or **[^{18}F]5f** were eluted into the outlet vial (V20) with reverse flow of DMSO (1 mL, syringe S3 (V24)).

3.2.2. Low-Activity ^{18}F-Labeling Experiments in the Precursors **6a–6f**

Using the GE FASTlab^{TM} synthesizer, an aliquot of [^{18}F]fluoride (150–200 MBq) was trapped on a Sep-Pak® Accell^{TM} Plus QMA Carbonate Plus Light cartridge (Waters, Milford, MA, USA) and

eluted with a solution of Kryptofix® 222 ($K_{2.2.2}$; 7.5 mg in 600 μL of MeCN) and K_2CO_3 (1.4 mg in 150 μL of H_2O). Upon azeotropic drying, a solution of the precursors **6a** (12.3 mg, 0.04 mmol), **6b** (12.3 mg, 0.04 mmol), **6c** (6.5 mg, 0.02 mmol), **6d** (12.9 mg, 0.04 mmol), **6e** (11.0 mg, 0.04 mmol), or **6f** (11.6 mg, 0.04 mmol) in MeCN (1 mL) was transferred to the dry [^{18}F]potassium fluoride/Kryptofix® 222 ([^{18}F]KF/$K_{2.2.2}$) complex and heated to 120 °C. After 5 min of ^{18}F-labeling and dilution of the reaction mixture with H_2O, the labeled compounds **[^{18}F]4a–[^{18}F]4f** were trapped on a Sep-Pak® C18 Plus Short cartridge (Waters, Milford, MA, USA). Subsequently, the ^{t}C18 cartridge was removed and the trapped crude products **[^{18}F]4a–[^{18}F]4f** were recovered to a 4 mL-vial *via* manual elution with MeCN (1 mL). The radiochemical yield (RCY) of the ^{18}F-labeling step was determined based on the activity of the recovered crude products **[^{18}F]4a–[^{18}F]4f**, on their radio-TLC and radio-UPLC purities, and the starting radioactivity, according to the following Equation (1):

$$\textit{RCY}\ (\%,\ \textit{d.c.}) = \frac{\textit{radioTLC purity}\ (\%)\ \times\ \textit{radioUPLC purity}\ (\%)\ \times\ \textit{activity of the solution of}\ [^{18}\mathbf{F}]\ \mathbf{4a}\text{–}[^{18}\mathbf{F}]\mathbf{4f}\ (\textit{d.c.})}{\textit{starting radioactivity}\ \times\ \mathbf{100}} \quad (1)$$

A solution containing $NaIO_4$ (153.9 mg, 0.072 mmol) and $RuCl_3{\cdot}xH_2O$ (3.4 mg, 0.016 mmol) in H_2O (1 mL) was transferred to the ^{t}C18 cartridge and the oxidation of the trapped crude products [^{18}F]4a–[^{18}F]4f (10–20 MBq) was carried out in solid-phase for 5 min at room temperature. Afterwards, the corresponding [^{18}F]difluoromethyl heteroaryl-sulfones **[^{18}F]5a–[^{18}F]5f** were manually eluted from the ^{t}C18 cartridge with MeCN (1 mL) to a 4 mL-vial. The RCY of the oxidation step was determined based on the activity of the crude products [^{18}F]4a–[^{18}F]4f and **[^{18}F]5a–[^{18}F]5f**, and on their radio-TLC and radio-UPLC purities, according to the following Equation (2):

$$\textit{RCY}\ (\%,\ \textit{d.c.}) = \frac{\textit{radioTLC purity}\ (\%)\ \times\ \textit{radioUPLC purity}\ (\%)\ \times\ \textit{activity of the solution of}\ [^{18}\mathbf{F}]\ \mathbf{5a}\text{–}[^{18}\mathbf{F}]\mathbf{5f}\ (\textit{d.c.})}{\textit{activity of the solution of}\ [^{18}\mathbf{F}]\ \mathbf{4a}\text{–}[^{18}\mathbf{F}]\mathbf{4f}\ \times\ \mathbf{100}} \quad (2)$$

The RCYs of ^{18}F-labeling and oxidation steps were decay-corrected at the SOS.

3.2.3. Isolation and Determination of the Molar Activity of **[^{18}F]5a**, **[^{18}F]5c**, and **[^{18}F]5f**

The fully automated radiosyntheses of the sulfones **[^{18}F]5a**, **[^{18}F]5c**, or **[^{18}F]5f** were accomplished on a commercially available FASTlab™ synthesizer (GE Healthcare, Chicago, IL, USA), using the optimized conditions for the labeling of precursors **6a** (12.3 mg, 0.04 mmol), **6c** (6.5 mg, 0.02 mmol), or **6f** (11.6 mg, 0.04 mmol), and for the oxidation of the labeled compounds **[^{18}F]4a**, **[^{18}F]4c**, and **[^{18}F]4f**. The molar activities of the sulfones **[^{18}F]5a**, **[^{18}F]5c**, and **[^{18}F]5f** were determined using an aliquot of each reformulated solution (3 μL). After UPLC injection, the radioactive peak of **[^{18}F]5a**, **[^{18}F]5c**, and **[^{18}F]5f** associated to the non-radioactive sulfones **5a**, **5c**, and **5f**, respectively, were collected and counted in an ionization chamber. The PDA UV area under the peak of the non-radioactive sulfones **5a**, **5c**, and **5f** at 258 nm, 290 nm, and 244 nm, respectively, enabled the determination of the corresponding amount (in μmol) of the **5a**, **5c**, and **5f** using the calibration curves described in the Supplementary Information (Figures S82–S84). The molar activities of **[^{18}F]5a**, **[^{18}F]5c**, and **[^{18}F]5f** were determined on the basis of the following Equation (3):

$$\textit{Molar activity}\ \left(\textit{GBq}{\cdot}\mu\textit{mol}^{-1}\right) = \frac{\textit{activity of the collected UPLC peak of}\ [^{18}\mathbf{F}]\ \mathbf{5a},\ \ [^{18}\mathbf{F}]\mathbf{5c},\ \ \textbf{or}\ [^{18}\mathbf{F}]\mathbf{5f}}{\textit{amount of}\ \mathbf{5a},\ \ \mathbf{5c},\ \ \textit{or}\ \mathbf{5f}\ \textit{associated to the radioactive peak}} \quad (3)$$

3.2.4. General Procedure for the C–H ^{18}F-Difluoromethylation of the Heteroarenes **7a–7g** with the [^{18}F]difluoromethyl heteroaryl-sulfones **[^{18}F]5a**, **[^{18}F]5c**, and **[^{18}F]5f**

A solution of the heteroarenes (0.02 mmol) and *fac*-$Ir^{III}(ppy)_3$ (0.05 mol% for **[^{18}F]5a**; 0.5 mol % for **[^{18}F]5c**; 0.1 mol % for **[^{18}F]5f**) in DMSO (200 μL) was prepared in a 4 mL-vial. Next, a solution of **[^{18}F]5a**, **[^{18}F]5c**, or **[^{18}F]5f** in DMSO (30–40 MBq, 50 μL) was added. The resulting mixture was injected in a 100 μL-microchip pumped with DMSO at a flow rate of 50 μL·min^{-1} (residence time: 2 min for

[^{18}F]5a), 25 μL·min^{-1} (residence time: 4 min for **[^{18}F]5c**) or 40 μL·min^{-1} (residence time: 2.5 min for **[^{18}F]5f**) and irradiated under blue LED (470 nm, 2 W), at a temperature of 35 °C. An aliquot of the reaction mixture containing the crude products **[^{18}F]8a**–**[^{18}F]8g** was then analyzed by radio-TLC and radio-UPLC for RCY determination, according to the following Equation (4):

$$\boldsymbol{RCY}\,(\%) = \frac{\boldsymbol{radioTLC\ purity}\ (\%)\ \times\ \boldsymbol{radioUPLC\ purity}\ (\%)}{\mathbf{100}} \tag{4}$$

4. Conclusions

In the present work, the two-step radiosyntheses of the [^{18}F]difluoromethyl heteroaryl-sulfones **[^{18}F]5a**, **[^{18}F]5c**, **[^{18}F]5f** was fully automated in the GE FASTlab^{TM} module. In conjunction with a semi-preparative HPLC purification procedure and formulation in a preconditioned Sep-Pak® C18 Plus Short Cartridge, the reagents **[^{18}F]5a**, **[^{18}F]5c**, **[^{18}F]5f** were isolated in reproducible 2.9 ± 0.1%, 5.7 ± 0.5%, and 8.0 ± 0.9% RCYs, respectively (decay-corrected at the SOS). The use of automated synthesizers in radiochemical processes involving the production of multiple GBq of labeled compounds is required to assure the minimization of the radiation exposure to workers.

The great probability of ^{18}F–^{19}F isotopic exchange still constitutes a major limitation in the preparation of [^{18}F]CF_2H–bearing compounds with high molar activity. The production of radiotracers with high molar activity is mandatory for PET imaging studies, especially for targeting low-density biomacromolecules. Starting from 125–150 GBq of [^{18}F]fluoride, this fully automated methodology enabled the preparation of the labeled compounds **[^{18}F]5a**, **[^{18}F]5c**, and **[^{18}F]5f** with improved molar activities (139 ± 17 GBq·μmol^{-1} for **[^{18}F]5a**, 62 ± 12 GBq·μmol^{-1} for **[^{18}F]5c**, and 113 ± 17 GBq·μmol^{-1} for **[^{18}F]5f**).

Interestingly, these newly synthesized compounds were revealed to be competent reagents for the C–H ^{18}F-difluoromethylation of the antiherpetic drug **7e** under the reaction conditions recently reported in our laboratories [37]. Still, none of the new reagents performed as good as the original sulfone **[^{18}F]1** in the radiosynthesis of the labeled compound **[^{18}F]8e**. Additionally, the sulfones **[^{18}F]5c** and **[^{18}F]5f** exhibited a lower reactivity towards the C–H ^{18}F-difluoromethylation of **7e**, in comparison with the sulfone **[^{18}F]1**. Overall, the introduction of molecular modifications in the structure of **[^{18}F]1** can modulate the reactivity of the resulting ^{18}F-difluoromethylating reagents, influencing the amount of photocatalyst and the residence time necessary to assure a complete C–H ^{18}F-difluoromethylation process. Delightfully, the labeled compounds **[^{18}F]5a**, **[^{18}F]5c**, and **[^{18}F]5f** were suitable for the developed flow photoredox C–H ^{18}F-difluoromethylation of a scope of heteroarenes, demanding a low amount of *fac*-$Ir^{III}(ppy)_3$ (0.05–0.5 mol %) and short residence times (2–4 min). Radical-scavenging experiments suggested the participation of radical intermediates in the present photocatalytic C–H ^{18}F-difluoromethylation reaction. To the best of our knowledge, the effectiveness of the non-radioactive references of **[^{18}F]5a**, **[^{18}F]5c**, and **[^{18}F]5f** as difluoromethylating reagents has never been described in visible light photoredox catalysis.

Overall, the described photocatalytic C–H ^{18}F-difluoromethylation protocol involving the newly synthesized reagents **[^{18}F]5a**, **[^{18}F]5c**, and **[^{18}F]5f** can be suitable for the development of novel [^{18}F]CF_2H-containing radioactive probes for PET imaging with improved molar activities.

Supplementary Materials: The following are available online http://www.mdpi.com/2073-4344/10/3/275/s1. Figures S1–S54. ^{1}H-, ^{13}C-, and ^{19}F-NMR spectrum of the compounds **4a**–**4f**, **5a**–**5f**, and **6a**–**6f**; Figure S55. TLC radio-chromatogram of the crude product **[^{18}F]4a**; Figures S56–S67: UPLC radio- and UV-chromatograms of the crude products **[^{18}F]4a**–**[^{18}F]4f** and their respective non-radioactive references (gradient A); Figure S68. TLC radio-chromatogram of the crude product **[^{18}F]5a**; Figures S69–S80: UPLC radio- and UV-chromatograms of the crude products **[^{18}F]5a**–**[^{18}F]5f** and their respective non-radioactive references (gradient A); Figure S81: Layout of the FASTlab^{TM} cassette for the radiosynthesis of the labeled compounds **[^{18}F]5a**, **[^{18}F]5c**, and **[^{18}F]5f**; Figures S82–S84: Calibration curve of the difluoromethyl heteroaryl-sulfones **5a**, **5c**, and **5f**; Figure S85: Instrument used for the C–H ^{18}F-difluoromethylation reaction of the heteroarenes (FlowStart Evo, FutureChemistry); Figure S86: TLC radio-chromatogram of the crude product **[^{18}F]8e**; Figures S87–S103: UPLC radio- and UV-chromatograms of

the crude products **[^{18}F]8a**–**[^{18}F]8g** and their respective non-radioactive references (gradient B); Tables S1 and S2: UPLC gradients for the analysis of the crude products **[^{18}F]4a**–**[^{18}F]4f**, **[^{18}F]5a**–**[^{18}F]5f**, and **[^{18}F]8a**–**[^{18}F]8g**; Table S3: Determination of the radio-TLC purity of the crude product **[^{18}F]4a**; Tables S4–S9: Determination of the radiochemical yield (%) of the synthesis of **[^{18}F]4a**–**[^{18}F]4f**; Table S10. Determination of the radio-TLC purity of the crude product **[^{18}F]5a**; Tables S11–S16: Determination of the radiochemical yield (%) of the synthesis of **[^{18}F]5a**–**[^{18}F]5f**; Tables S17–S22: Determination of the radiochemical yield (%) of the synthesis of **[^{18}F]5a**–**[^{18}F]5f** from the precursors **6a**–**6f**; Table S23: Location of the reagents, solvents, and materials in the manifold of the FASTlab^{TM} cassette; Tables S24–S26: Determination of the radiochemical yield (%) of the synthesis of **[^{18}F]5a**, **[^{18}F]5c**, and **[^{18}F]5f** from the precursors **6a**, **6c**, and **6f**, respectively; Tables S27–S29: Determination of the molar activity of **[^{18}F]5a**, **[^{18}F]5c**, and **[^{18}F]5f**; Table S30: Determination of the radio-TLC purity of the crude product **[^{18}F]8e**; Table S31–S51: Determination of the radiochemical yield (%) of the synthesis of **[^{18}F]8a**–**[^{18}F]8g** using the reagents **[^{18}F]5a**, **[^{18}F]5c**, and **[^{18}F]5f**.

Author Contributions: Conceptualization, C.G. and A.L.; investigation, A.L.P.L., L.T., B.L., P.P., J.M., and C.L.; resources, B.L., P.P., J.M., C.L., J.-C.M., C.G, and A.L.; writing—original draft preparation, A.L.P.L. and L.T.; writing—review and editing, A.L.P.L., L.T., B.L., P.P., J.M., C.L., C.G., and A.L.; supervision, C.G. and A.L.; project administration, C.G. and A.L.; funding acquisition, C.G. and A.L. All authors have read and agreed to the published version of the manuscript.

Funding: This work was supported by funding from the European Union's Horizon 2020 research and innovation program under the Marie Skłodowska-Curie grant agreement No. 675071 (ISOTOPICS) and from the University of Liège.

Conflicts of Interest: The authors declare no conflict of interest. The founding sponsors had no role in the design of the study; in the collection, analyses, or interpretation of data; in the writing of the manuscript, and in the decision to publish the results.

References

1. Le Bars, D. Fluorine-18 and medical imaging: Radiopharmaceuticals for positron emission tomography. *J. Fluorine Chem.* **2006**, *127*, 1488–1493. [CrossRef]
2. Even-Sapir, E.; Mishani, E.; Flusser, G.; Metser, U. ^{18}F-Fluoride positron emission tomography and positron emission tomography/computed tomography. *Semin. Nucl. Med.* **2007**, *37*, 462–469. [CrossRef]
3. Banister, S.; Roeda, D.; Dollé, F.; Kassiou, M. Fluorine-18 chemistry for PET: A concise introduction. *Curr. Radiopharm.* **2010**, *3*, 68–80. [CrossRef]
4. Varlow, C.; Szames, D.; Dahl, K.; Bernard-Gauthier, V.; Vasdev, N. Fluorine-18: An untapped resource in inorganic chemistry. *Chem. Commun.* **2018**, *54*, 11835–11842. [CrossRef]
5. Shukla, A.K.; Kumar, U. Positron emission tomography: An overview. *J. Med. Phys.* **2006**, *31*, 13–21. [CrossRef]
6. Lin, M.; Shon, I.H.; Lin, P. Positron emission tomography: Current status and future challenges. *Intern. Med. J.* **2010**, *40*, 19–29. [CrossRef] [PubMed]
7. Vaquero, J.J.; Kinahan, P. Positron emission tomography: Current challenges and opportunities for technological advances in clinical and preclinical imaging systems. *Annu. Rev. Biomed. Eng.* **2015**, *17*, 385–414. [CrossRef] [PubMed]
8. El-Galaly, T.C.; Gormsen, L.C.; Hutchings, M. PET/CT for staging; Past, present, and future. *Semin. Nucl. Med.* **2018**, *48*, 4–16. [CrossRef] [PubMed]
9. Miller, P.W.; Long, N.J.; Vilar, R.; Gee, A.D. Synthesis of ^{11}C, ^{18}F, ^{15}O, and ^{13}N radiolabels for positron emission tomography. *Angew. Chem. Int. Ed.* **2008**, *47*, 8998–9033. [CrossRef] [PubMed]
10. Gu, Y.; Huang, D.; Liu, Z.; Huang, J.; Zeng, W. Labeling strategies with F-18 for positron emission tomography imaging. *Med. Chem.* **2011**, *7*, 334–344. [CrossRef]
11. Ying, L. ^{18}F-Labeling techniques for positron emission tomography. *Sci. China Chem.* **2013**, *56*, 1682–1692.
12. Brooks, A.F.; Topczewski, J.J.; Ichiishi, N.; Sanford, M.S.; Scott, P.J.H. Late-stage [^{18}F]fluorination: New solutions to old problems. *Chem. Sci.* **2014**, *5*, 4545–4553. [CrossRef] [PubMed]
13. Jacobson, O.; Kiesewetter, D.O.; Chen, X. Fluorine-18 radiochemistry, labeling strategies and synthetic routes. *Bioconjugate Chem.* **2015**, *26*, 1–18. [CrossRef] [PubMed]
14. Preshlock, S.; Tredwell, M.; Gouverneur, V. ^{18}F-Labeling of arenes and heteroarenes for applications in positron emission tomography. *Chem. Rev.* **2016**, *116*, 719–766. [CrossRef] [PubMed]
15. Van der Born, D.; Pees, A.; Poot, A.J.; Orru, R.V.A.; Windhorst, A.D.; Vugts, D.J. Fluorine-18 labelled building blocks for PET tracer synthesis. *Chem. Soc. Rev.* **2017**, *46*, 4709–4773. [CrossRef] [PubMed]

16. Krishnan, H.S.; Ma, L.; Vasdev, N.; Liang, S.H. ^{18}F-Labeling of sensitive biomolecules for positron emission tomography. *Chem. Eur. J.* **2017**, *23*, 15553–15577. [CrossRef]
17. Coenen, H.H.; Ermert, J. ^{18}F-Labeling innovations and their potential for clinical application. *Clin. Transl. Imaging* **2018**, *6*, 169–193. [CrossRef]
18. Krüll, J.; Heinrich, M.R. [^{18}F] Fluorine-labeled pharmaceuticals: Direct aromatic fluorination compared to multi-step strategies. *Asian, J. Org. Chem.* **2019**, *8*, 576–590. [CrossRef]
19. Deng, X.; Rong, J.; Wang, L.; Vasdev, N.; Zhang, L.; Josephson, L.; Liang, S.H. Chemistry for positron emission tomography: Recent advances in ^{11}C-, ^{18}F-, ^{13}N-, and ^{15}O-labeling reactions. *Angew. Chem. Int. Ed.* **2019**, *58*, 2580–2605. [CrossRef]
20. Meanwell, N.A. Fluorine and fluorinated motifs in the design and application of bioisosteres for drug design. *J. Med. Chem.* **2018**, *61*, 5822–5880. [CrossRef]
21. Erickson, J.A.; McLoughlin, J.I. Hydrogen bond donor properties of the difluoromethyl group. *J. Org. Chem.* **1995**, *60*, 1626–1631. [CrossRef]
22. Zafrani, Y.; Yeffet, D.; Sod-Moriah, G.; Berliner, A.; Amir, D.; Marciano, D.; Gershonov, E.; Saphier, S. Difluoromethyl bioisostere: Examining the "lipophilic hydrogen bond donor" concept. *J. Med. Chem.* **2017**, *60*, 797–804. [CrossRef] [PubMed]
23. Sessler, C.D.; Rahm, M.; Becker, S.; Goldberg, J.M.; Wang, F.; Lippard, S.J. CF_2H, a hydrogen bond donor. *J. Am. Chem. Soc.* **2017**, *139*, 9325–9332. [CrossRef] [PubMed]
24. Zafrani, Y.; Sod-Mariah, G.; Yeffet, D.; Berliner, A.; Amir, D.; Marciano, D.; Elias, S.; Katalan, S.; Ashkenazi, N.; Madmon, M.; et al. CF_2H, a functional group-dependent hydrogen-bond donor: Is it a more or less lipophilic bioisostere of OH, SH, and CH_3? *J. Med. Chem.* **2019**, *62*, 5628–5637. [CrossRef] [PubMed]
25. Rong, J.; Ni, C.; Hu, J. Metal-catalyzed direct difluoromethylation reactions. *Asian J. Org. Chem.* **2017**, *6*, 139–152. [CrossRef]
26. Yerien, D.E.; Barata-Vallejo, S.; Postigo, A. Difluoromethylation reactions of organic compounds. *Chem. Eur. J.* **2017**, *23*, 14676–14701. [CrossRef] [PubMed]
27. Feng, Z.; Xiao, Y.-L.; Zhang, X. Transition-metal (Cu, Pd, Ni)-catalyzed difluoroalkylation via cross-coupling with difluoroalkyl halides. *Acc. Chem. Res.* **2018**, *51*, 2264–2278. [CrossRef]
28. Lemos, A.; Lemaire, C.; Luxen, A. Progress in difluoroalkylation of organic substrates by visible light photoredox catalysis. *Adv. Synth. Catal.* **2019**, *361*, 1500–1537. [CrossRef]
29. Koike, T.; Akita, M. Recent progress in photochemical radical di- and mono-fluoromethylation. *Org. Biomol. Chem.* **2019**, *17*, 5413–5419. [CrossRef]
30. Levi, N.; Amir, D.; Greshonov, E.; Zafrani, Y. Recent progress on the synthesis of CF_2H-containing derivatives. *Synthesis* **2019**, *51*, 4549–4567. [CrossRef]
31. Wagner, K.; Kraatz, U.; Kugler, M.; Schrage, H.; Uhr, H. Benzazole derivatives with microbiocidal properties. Ger. Offen. DE 19523447 A1 19970102, 1997.
32. Mizuta, S.; Stenhagen, I.S.R.; O'Duill, M.; Wolstenhulme, J.; Kirjavainen, A.K.; Forsback, S.J.; Tredwell, M.; Sandford, G.; Moore, P.R.; Huiban, M.; et al. Catalytic decarboxylative fluorination for the synthesis of tri- and difluoromethyl arenes. *Org. Lett.* **2013**, *15*, 2648–2651. [CrossRef] [PubMed]
33. Verhoog, S.; Pfeifer, L.; Khotavivattana, T.; Calderwood, S.; Collier, T.L.; Wheelhouse, K.; Tredwell, M.; Gouverneur, V. Silver-mediated ^{18}F-labeling of aryl-CF_3 and aryl-CHF_2 with ^{18}F-fluoride. *Synlett* **2016**, *27*, 25–28.
34. Shi, H.; Braun, A.; Wang, L.; Liang, S.H.; Vasdev, N.; Ritter, T. Synthesis of ^{18}F-difluoromethylarenes from aryl (pseudo) halides. *Angew. Chem. Int. Ed.* **2016**, *55*, 10786–10790. [CrossRef]
35. Yuan, G.; Wang, F.; Stephenson, N.A.; Wang, L.; Rotstein, B.H.; Vasdev, N.; Tang, P.; Liang, S.H. Metal-free ^{18}F-labeling of aryl-CF_2H *via* nucleophilic radiofluorination and oxidative C–H activation. *Chem. Commun.* **2017**, *53*, 126–129. [CrossRef] [PubMed]
36. Sap, J.B.I.; Wilson, T.C.; Kee, C.W.; Straathof, N.J.W.; amEnde, C.W.; Mukherjee, P.; Zhang, L.; Genicot, C.; Gouverneur, V. Synthesis of ^{18}F-difluoromethylarenes using aryl boronic acids, ethyl bromofluoroacetate and [^{18}F]fluoride. *Chem. Sci.* **2019**, *10*, 3237–3241. [CrossRef] [PubMed]
37. Trump, L.; Lemos, A.; Lallemand, B.; Pasau, P.; Mercier, J.; Lemaire, C.; Luxen, A.; Genicot, C. Late-stage ^{18}F-difluoromethyl labeling of *N*-heteroaromatics with high molar activity. *Angew. Chem. Int. Ed.* **2019**, *58*, 13149–13154. [CrossRef] [PubMed]

38. Trump, L.; Lemos, A.; Jacq, J.; Pasau, P.; Lallemand, B.; Mercier, J.; Genicot, C.; Luxen, A.; Lemaire, C. Development of a general automated flow photoredox ^{18}F-difluoromethylation of *N*-heteroaromatics in an AllinOne synthesizer. *Org. Process Res. Dev.* **2020**. [CrossRef]
39. Rong, J.; Deng, L.; Tan, P.; Ni, C.; Gu, Y.; Hu, J. Radical fluoroalkylation of isocyanides with fluorinated sulfones by visible-light photoredox catalysis. *Angew. Chem. Int. Ed.* **2016**, *55*, 2743–2747. [CrossRef]
40. Fu, W.; Han, X.; Zhu, M.; Xu, C.; Wang, Z.; Ji, B.; Hao, X.-Q.; Song, M.-P. Visible-light-mediated radical oxydifluoromethylation of olefinic amides for the synthesis of CF_2H-containing heterocycles. *Chem. Commun.* **2016**, *52*, 13413–13416. [CrossRef]
41. Zou, G.; Wang, X. Visible-light induced di- and trifluoromethylation of *N*-benzamides with fluorinated sulfones for the synthesis of CF_2H/CF_3-containing isoquinolinediones. *Org. Biomol. Chem.* **2017**, *15*, 8748–8751. [CrossRef] [PubMed]
42. Zhu, M.; Fu, W.; Wang, Z.; Xu, C.; Ji, B. Visible-light-mediated direct difluoromethylation of alkynoates: Synthesis of 3-difluoromethylated coumarins. *Org. Biomol. Chem.* **2017**, *15*, 9057–9060. [CrossRef] [PubMed]
43. Zhu, M.; Fu, W.; Guo, W.; Tian, Y.; Wang, Z.; Xu, C.; Ji, B. Visible-light-induced radical di- and trifluoromethylation of β, γ-unsaturated oximes: Synthesis of di- and trifluoromethylated isoxazolines. *Eur. J. Org. Chem.* **2019**, *2019*, 1614–1619. [CrossRef]
44. Zhu, M.; You, Q.; Li, R. Synthesis of CF_2H-containing oxindoles via hotoredox-catalyzed radical difluoromethylation and cyclization of *N*-arylacrylamides. *J. Fluorine Chem.* **2019**. [CrossRef]
45. Sun, H.; Jiang, Y.; Yang, Y.-S.; Li, Y.-Y.; Li, L.; Wang, W.-X.; Feng, T.; Li, Z.-H.; Liu, J.-K. Synthesis of difluoromethylated 2-oxindoles and quinoline-2,4-dione via visible light-induced tandem radical cyclization of *N*-arylacrylamides. *Org. Biomol. Chem.* **2019**, *17*, 6629–6638. [CrossRef] [PubMed]
46. Arai, Y.; Tomita, R.; Ando, G.; Koike, T.; Akita, M. Oxydifluoromethylation of alkenes by photoredox catalysis: Simple synthesis of CF_2H-containing alcohols. *Chem. Eur. J.* **2016**, *22*, 1262–1265. [CrossRef]
47. Carbonnel, E.; Besset, T.; Poisson, T.; Labar, D.; Pannecoucke, X.; Jubault, P. ^{18}F-Fluoroform: A ^{18}F-trifluoromethylating agent for the synthesis of $SCF_2{}^{18}$F-aromatic derivatives. *Chem. Commun.* **2017**, *53*, 5706–5709. [CrossRef]
48. O'Brien, J.J.; Campoli-Richards, D.M. Acyclovir. An updated review of its antiviral activity, pharmacokinetic properties and therapeutic efficacy. *Drugs* **1989**, *37*, 233–309.
49. Fenton, C.; Keating, G.M.; Lyseng-Williamson, K.A. Moxonidine. A review of its use in essential hypertension. *Drugs* **2006**, *66*, 477–496. [CrossRef]
50. Frampton, J.E.; Brogden, R.N. Pentoxifylline (Oxpentifylline). A review of its therapeutic efficacy in the management of peripheral vascular and cerebrovascular disorders. *Drugs Aging* **1995**, *7*, 480–503. [CrossRef]
51. Sakamoto, R.; Kashiwagi, H.; Marouka, K. The direct C–H difluoromethylation of heteroarenes based on the photolysis of hypervalent iodine(III) reagents that contain difluoroacetoxy ligands. *Org. Lett.* **2017**, *19*, 5126–5129. [CrossRef] [PubMed]
52. Lemaire, C.; Libert, L.; Franci, X.; Genon, J.-L.; Kuci, S.; Giacomelli, F.; Luxen, A. Automated production at the curie level of no-carrier-added 6-[^{18}F]fluoro-L-dopa and 2-[^{18}F]fluoro-L-tyrosine on a FASTlab synthesizer. *J. Label. Compd. Radiopharm.* **2015**, *58*, 281–290. [CrossRef] [PubMed]

© 2020 by the authors. Licensee MDPI, Basel, Switzerland. This article is an open access article distributed under the terms and conditions of the Creative Commons Attribution (CC BY) license (http://creativecommons.org/licenses/by/4.0/).